TIDAL FORCE AND TORQUE ON THE CRUST OF NEUTRON STAR

By

Asfaw Merid

SUBMITTED IN PARTIAL FULFILLMENT OF THE
REQUIREMENTS FOR THE DEGREE OF
MASTER OF SCIENCE IN PHYSICS
AT
ADDIS ABABA UNIVERSITY
ADDIS ABABA, ETHIOPIA
JUNE 2013

ADDIS ABABA UNIVERSITY
DEPARTMENT OF
PHYSICS

Signed by the Examining Committee:

Examiner:Prof. Ashok.V.Gholap Signature:_____Date:_____

Examiner:Prof.A.K. Chaubey Signature:_____Date:_____

Advisor: Dr. Legesse Wetro Signature:_____Date:_____

ADDIS ABABA UNIVERSITY

Date: **June 2013**

Author: **Asfaw Merid**

Title: **TIDAL FORCE AND TORQUE ON THE CRUST OF NEUTRON STAR**

Department: **Physics**

Degree: **M.Sc.** Convocation: **June** Year: **2013**

Permission is herewith granted to Addis Ababa University to circulate and to have copied for non-commercial purposes, at its discretion, the above title upon the request of individuals or institutions.

Signature of Author

DEDICATED TO

My Grand Mother Emuhay Bezienash Lakew.

TATEY:

You are sunlight in my day,

You are the moon I see far away.

You are the one that makes troubles be gone.

You are the one who taught me life,

How not to fight, and what is right.

You are the words inside my song,

You are my love, my life,my mom.

You are the one who cares for me,

You are the eyes that help me see.

You are the one who knows me best,

When it's time to have fun and time to rest.

You are the one who has helped me to dream,

You hear my heart and you hear my screams.

Afraid of life but looking for love,

I'm blessed for God sent you from above.

Table of Contents

List of Figures

Abstract

A neutron star core superfluid rotates at a different rate to that of the crust, while spinning down at the same steady-state rate as the rest of the star, because of the assumed pinning between the superfluid vortices and the inner crust. We find that the magnitude of this rotational lag changes with time and also depends on the distance from the rotation axis; the core superfluid supports an evolving pattern of differential rotation. We predicted change of the lag might occur as discrete events which could result in a sudden rise of the spin frequency of the crust of a neutron star, as is observed in glitches in radio pulsars. Glitches are believed to have been caused by break aways of pinned vortices.This new possibility for the triggering cause of glitches in radio pulsars is further supported by an estimate of the total predicted excess angular momentum reservoir of the core superfluid. The model seems to offer resolutions for some other aspects of the observational data on glitches. The goal of this project is to show the tidal force effect on the differential motion of the crust with respect to the core of the neutron star could lead to the reduction of glitch frequencies and eventually produced gravitational locking between the core and the crust of a neutron star.

Acknowledgements

First and foremost I thank Almighty God, my strength and power. What can I give Him in return?

I would like to express my sincere thanks to my advisor and instructor Dr. Legesse Wetro for his guidance, assistance, and contribution of valuable suggestions. His beautiful lectures has made a deep impression on me.

I wish to thank David and Angela Williams and their family for their moral, material and financial support.Without their invaluable support my work could not go beyond being a dream.

Last but not least, I thank my family and friends for their encouragement and support.

Introduction

In this thesis we discuss the rotational dynamics of neutron stars taking into account also the effects of the pinning of the core vortices onto the crust of the star. Any study of the rotational dynamics of these stars would naturally concern atleast partly ,if not completely,to the phenomenon of glitches. The observed glitches in radio pulsars provide unique "laboratory tests" for the ideas about the interior of neutron stars. A brief review of the important aspects of the observational data on glitches and the related theoretical models is therefore discussed.

One of the most striking features of a pulsar is its extreme regularity in its period. From time to time, this regular and predictable period abruptly changes in what is known as a glitch. It is by studying these glitches that we obtain most important information about the internal makeup of a neutron star, and therefore about the nature of nuclear matter at high densities.

Glitches are observed in radio pulsars as sudden changes in the rotation frequency of the crust,Ω_c , with observed values of the jump in the range$10^{-9} \leq \Delta\Omega_c/\Omega_c \leq 10^{-6}$. In younger pulsars the jump in Ω_c is also accompanied by an increase $\Delta\dot{\Omega}_c$ in the observe spin-down rate $\dot{\Omega}_c$ of the crust, which causes a recovery or relaxation back towards the pre- glitch behaviour of Ω_c over timescales of days to years.It is generally understood that glitches should be caused by mechanisms related to the internal structure of the star.The two generally accepted mechanisms for glitches thus invoke starquakes (Baym et al. 1969) and unpinning of the vortices of a superfluid component in the crust (Anderson Itoh 1975). In the latter mechanism, which is more relevant to the present discussion, a

sudden release and rapid outward motion of a large number of otherwise pinned vortices act as the source of the excess angular momentum, which is transferred to the crust, hence causing the observed jump in Ω_c. Suggested mechanisms for the sudden release of a large number of initially pinned vortices include catastrophic unpinning due to an intrinsic instability, breaking down of the crustal lattice by magnetic stresses, and thermal instability resulting in an increase in the mutual friction between the vortices and the superfluid (Anderson and Itoh 1975). The coupled evolution of the neutron vortices and the proton fluxoids has nevertheless been discussed in various other respects, including its role in the post-glitch relaxation and also in driving glitches indirectly through crustal effects (Ruderman et al. 1998). Our aim here is to point at a so far unexplained property of the rotational evolution of the core superfluid that might serve to reduce the frequency of glitches, directly. This is suggested based on the calculated long-term reduction of the rotational lag between the superfluid core and the crust by tidal torque.In due process the latter will come to a state of corotation with the crust, on a time-scales larger than 1.58×10^3years. with the crust,so that after this time the pulsar will not show any glitch. The thesis is organized as follows:In chapter-one we discuss about the tidal interactions which leads to a discussion on tidal force in Newtonian as well as general relativistic frames and geodetic precession,In chapter-two we give a brief discussion on neutron star(its formation,structure ,composition,...etc),In chapter-three we give a detailed discussion on Superfluidity in Neutron Stars and Glitch diagnostics In chapter-four we discuss about the gravitoelectromagnetic and Lense-Thirring effect and In chapter-five (the last chapter), we discuss our results and lastly we put our conclusion.

Chapter 1

Tides

Tides are the manifestations of a gradient of the gravitational force field induced by a mass above an extended body or a system of particles. The study of tidal fields in the most simple cases can be done by analytically approximating the potential field of a non spherical mass distribution by a spherical (that is, a point mass) potential.

1.1 The Newtonian Tidal Forces

The Newtonian tidal tensor is a useful tool for the study of tidal fields. Because the Newtonian tidal tensor is frequently employed in a somewhat obscure way in the literature, it is useful to recall some of its properties and see how it naturally leads to the common tidal textbook formalism.

Once a coordinate system and a frame of reference is defined (typically with its origin at the mass distributions center of mass) and given the mass distributions gravitational force field F(R),the tidal forces arise as the manifestation of the gradient ∇F(R) [1]. The tidal force induced by a mass distribution on another body or another system of particles is defined as the difference between the gravitational force that the mass exerts at that point, and the mean gravitational force <F> it exerts on the whole body or system

$$F_t(R) = F(R) - < F > \tag{1.1.1}$$

It can be shown that the mean gravitational force acting on the tidally perturbed system is equivalent to the force acting at its center of mass, $R_{cm}, F(R_{cm})$. Hence without any

loss of generality, we can write the tidal fields as

$$F_t(R) = \Delta F = F(R) - F(R_{cm}) \tag{1.1.2}$$

Once the gravitational force field is expressed in terms of the potential Φ(R) as $F(R) = -\nabla\Phi(R)$, F_t is completely determined if we introduce the second rank symmetric Newtonian tidal force tensor,

$$T_{ij} = -\frac{\partial^2 \Phi}{\partial x_i \partial x_j} \tag{1.1.3}$$

with i , j = 1, 2, 3 and x_1 = x, x_2 = y, x_3 = z; T_{ij} is symmetric due to the conservative character of gravitational fields. If we use Einstein's summation convention, the components of the tidal force F_t in its differential form is

$$dF_{t_{x_i}} = \frac{\partial F_i}{\partial x_j} dx^j = -\frac{\partial^2 \Phi}{\partial x_i \partial x_j} dx^j = T_{ij} dx^j \tag{1.1.4}$$

The negative of the trace of T_{ij} gives Poissons equation, which relates the potential Φ to the mass density ρ

$$\nabla^2 \Phi = \frac{\partial^2 \Phi}{\partial x^2} + \frac{\partial^2 \Phi}{\partial y^2} + \frac{\partial^2 \Phi}{\partial z^2} = 4\pi\rho(x, y, z) \tag{1.1.5}$$

Poissons equation is nothing more than a trace invariant quantity of the tidal tensor matrix.

The Newtonian tidal tensor T_{ij} is the classical counterpart of the more general fourth rank Riemann space_time curvature tensor of general relativity, which is why it is called Newtonian.

To become better acquainted with the procedure of the next sections it is be useful to recover the main concepts associated with the most typical tidal perturbation that induced by the spherical potential of a point mass $\Phi(r) = \frac{GM}{r}$ [2]. Because it is a real symmetric matrix, there must be a frame of reference for which T^{ij} is diagonal.If we choose a frame of reference where the z-axis passes through the particles position, corresponding to the radial spherical coordinate, that is, (x =0,y = 0, z = r), then T_{ij} is diagonal and

becomes

$$T_{ij} = G\begin{pmatrix} -\frac{M}{z^3} & 0 & 0 \\ 0 & -\frac{M}{z^3} & 0 \\ 0 & 0 & \frac{2M}{z^3} \end{pmatrix} \equiv G\begin{pmatrix} -\frac{M}{r^3} & 0 & 0 \\ 0 & -\frac{M}{r^3} & 0 \\ 0 & 0 & \frac{2M}{r^3} \end{pmatrix} \tag{1.1.6}$$

From Eq. (4) we obtain

$$dF^{ij}_{t_x} = -\frac{Gm}{r^3}dx \tag{1.1.7}$$

$$dF^{ij}_{t_y} = -\frac{Gm}{r^3}dy \tag{1.1.8}$$

$$dF^{ij}_{t_z} = \frac{2Gm}{r^3}dz \tag{1.1.9}$$

The radial tidal force represents a change in the absolute value of the force vector, and the longitudinal and latitudinal vectors represent an angular variation of the components of the central force:

$$T_{xx} = T_{yy} = -\frac{Gm}{r^3} = -\frac{F(r)}{r}$$
$$T_{zz} = \frac{2Gm}{r^3} = \frac{\partial F(r)}{\partial r} \tag{1.1.10}$$

The tidal force given by equation (1.1.7),(1.1.8),and (1.1.9) satisfies the identity

$$\frac{\partial F_x}{\partial x} + \frac{\partial F_y}{\partial y} + \frac{\partial F_z}{\partial z} = -\frac{GM}{r^3} - \frac{GM}{r^3} + \frac{2GM}{r^3} = 0 \tag{1.1.11}$$

That is the tidal force has zero divergence. This result hold in general for gravitational field in empty region of space and can be expressed as

$$\frac{\partial F^k}{\partial x^k} = -\frac{\partial}{\partial x^k}\left(x^l \frac{\partial^2 \Phi}{\partial x^k \partial^l}\right) = -\delta^l_k \frac{\partial^2 \Phi}{\partial x^k \partial x^l} = -\frac{\partial^2 \Phi}{\partial x^k \partial x^k} = 0 \tag{1.1.12}$$

The last equation hold true because in empty space, the gravitational potential satisfies the laplace equation. But in the presence of a mass density ,the divergence of the tidal force is given by

$$\frac{\partial F^k}{\partial x^k} = 4\pi G\rho \tag{1.1.13}$$

As we will see later the tidal force given by general relativity (contained in equation of geodesic deviation) depend on the velocity of the particle with respect to the reference

point . However, the general relativity tidal force agrees with above Newton value in the limit of weak gravitational field ($\frac{Gm}{r}$) and low speed ($v \ll c$).

The detection of tidal field can be explained by means of the following practical example; suppose the astronauts place a freely spinning rigid body in the spacecraft as shown in the figure 1.1. The tidal force will exert a torque on the rod and give it an angular acceleration.For the tidal field given by equation(1.1.7),(1.1.8),and (1.1.9), the torque about the x-axis is

$$\tau_x = \int \left[y\left(2z\frac{GM}{r_0^3}\right) - z\left(-y\frac{GM}{r_0^3}\right)\right] dm = \frac{3GM}{r_0^3}\int yz dm = \frac{3GM}{r_0^3}\left(-I_{yz}\right) \quad (1.1.14)$$

Here $I_{yz} = I^{23}$ is the y-z component of the moment of inertia tensor defined by,[2]

$$I^{\kappa\iota} = \int \left(r^2\delta^\kappa_\iota - x^\kappa x^\iota\right) dm \quad (1.1.15)$$

Where δ^κ_ι is the Kronecker delta. Expression similar to 1.1.14 can be found for the torques about the y and z axes. Generally the torque exerted by an arbitrary tidal field $R^\kappa_{0\iota 0}$ on a body with an inertia tenser $I^{\iota s}$ is given by

$$\tau^n = c^2 \Sigma \epsilon^{n\kappa\iota} R^\kappa_{0\iota 0}\left(-I^{\iota s} + \frac{1}{3}\delta^\iota_s I^{rr}\right) \quad (1.1.16)$$

where $\epsilon^{\kappa\iota m}$ is defined as follows

$$\epsilon^{123} = \epsilon^{231} = \epsilon^{312} = 1$$

$$\epsilon^{321} = \epsilon^{213} = \epsilon^{132} = -1 \quad (1.1.17)$$

with all other components zero . If no other forces act equation 1.1.16 implies that the x-component of the spin of the rigid body changes at a rate

$$\frac{dS_x}{dt} = -\frac{3GM}{r_0^3} I_{yz} \quad (1.1.18)$$

Similar formula can be obtained for the rate of the change of the other component of the spin. This rate change of the spin can serve as a measure of the tidal field.

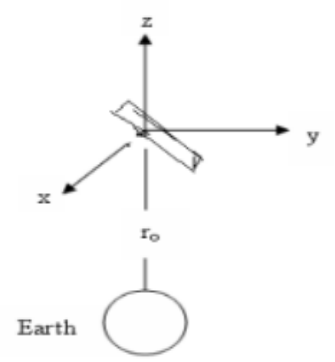

Figure 1.1: A rigid rod in free fall, instantaneously at rest at the origin of the coordinates

1.2 Relativistic Tidal Force

We may now ask what is the effect of the perturbation on matter. The easiest way to understand the action of gravitational waves is to consider the relative motion of two nearby test particles in free fall[4]. A free-falling test particle obeys the geodesic equation,

$$\frac{d^2x^\mu}{d\tau^2} + \Gamma^\mu_{\nu\rho}(x)\frac{dx^\nu}{d\tau}\frac{dx^\rho}{d\tau} = 0 \tag{1.2.1}$$

To see how we can derive the form of the Riemann_Christoffel tensor via computing the deviation of two neighbouring geodesics in our manifold, consider two test particles (labelled 1 and 2) moving along nearby geodesics. Let $\xi^\mu(\tau)$ denote the (infinitesimal) separation of the particles at proper time τ , so that

$$x^\mu_2(\tau) = x^\mu_1(\tau) + \xi^\mu(\tau) \tag{1.2.2}$$

Now the worldline of each particle is described by the geodesic equation, i.e.

$$\frac{d^2x^\mu_1}{d\tau^2} + \Gamma^\mu_{\alpha\beta}(x_1)\frac{dx^\alpha_1}{d\tau}\frac{dx^\beta_1}{d\tau} = 0, \tag{1.2.3}$$

and

$$\frac{d^2x^\mu_2}{d\tau^2} + \Gamma^\mu_{\alpha\beta}(x_2)\frac{dx^\alpha_2}{d\tau}\frac{dx^\beta_2}{d\tau} = 0 \tag{1.2.4}$$

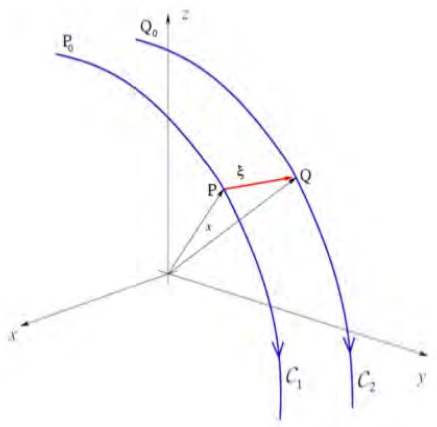

Figure 1.2: The trajectories of two free-falling particles in a gravitational field Φ. The three-vector ξ measures the distance between the two particles and is a function of time.

Note also that, by Taylor expanding the Christoffel symbols at x_1 in terms of ξ , we may write

$$\Gamma^{\mu}_{\alpha\beta}(x_2) = \Gamma^{\mu}_{\alpha\beta}(x_1 + \xi) = \Gamma^{\mu}_{\alpha\beta}(x_1) + \Gamma^{\mu}_{\alpha\beta}, \gamma\xi^{\gamma} \tag{1.2.5}$$

Subtracting equation (1.2.3) from equation (1.2.4), substituting from equation (1.2.5) and keeping only terms up to first order in ξ yields the following equation for the acceleration of ξ (dropping the subscript 1)

$$\frac{d^2\xi^{\mu}}{d\tau^2} + \Gamma^{\mu}_{\alpha\beta}\upsilon^{\alpha}\frac{d\xi^{\beta}}{d\tau} + \Gamma^{\mu}_{\alpha\beta}\upsilon^{\beta}\frac{d\xi^{\alpha}}{d\tau} + \Gamma^{\mu}_{\alpha\beta}, \gamma\xi^{\gamma}\upsilon^{\alpha}\upsilon^{\beta} = 0 \tag{1.2.6}$$

where we have used the fact that $\upsilon^{\alpha} \equiv \frac{dx^a}{d\tau}$. Equation (1.2.6) is not a tensor equation, since the Christoffel symbols and their derivatives do not transform as a tensor. We can develop the corresponding covariant expression, however, by taking covariant derivatives of the geodesic deviation. To this end, consider the covariant derivative of a general vector field $\mathbf{A}$ along a geodesic with tangent vector $\mathbf{v} \equiv \frac{d\mathbf{x}}{d\tau}$. We write this covariant derivative as $\nabla_{\mathbf{v}}\mathbf{A}$,or in component form, introducing the covariant operator $\frac{D}{D\tau}$

$$\frac{DA^{\mu}}{D\tau} = \frac{dA^{\mu}}{d\tau} + \Gamma^{\mu}_{\alpha\beta}A^{\alpha}\frac{dx^{\beta}}{d\tau}, \tag{1.2.7}$$

Now consider the second covariant derivative of the geodesic deviation, evaluated along the geodesic followed by test particle 1. From equation (1.2.7) in component form

$$\frac{D\xi^\mu}{D\tau} = \frac{d\xi^\mu}{d\tau} + \Gamma^\mu_{\alpha\beta}\xi^\alpha \frac{dx^\beta}{d\tau}, \tag{1.2.8}$$

It then follows that

$$\frac{D^2\xi^\mu}{D\tau^2} = \frac{D}{D\tau}\left(\frac{D\xi^\mu}{D\tau}\right) = \frac{d}{d\tau}\left(\frac{D\xi^\mu}{D\tau}\right) + \Gamma^\mu_{\sigma\delta}\frac{D\xi^\sigma}{D\tau}v^\delta, \tag{1.2.9}$$

Substituting again for $\frac{D\xi^\mu}{D\tau}$ we obtain

$$\frac{D^2\xi^\mu}{D\tau^2} = \frac{d}{d\tau}\left(\frac{d\xi^\mu}{d\tau} + \Gamma^\mu_{\alpha\beta}\xi^\alpha v^\beta\right) + \Gamma^\mu_{\sigma\delta}\left(\frac{d\xi^\sigma}{d\tau} + \Gamma^\sigma_{\alpha\beta}\xi^\alpha v^\beta\right)v^\delta, \tag{1.2.10}$$

Now, applying the product rule for differentiation

$$\frac{d}{d\tau}\left(\Gamma^\mu_{\alpha\beta}\xi^\alpha v^\beta\right) = \Gamma^\mu_{\alpha\beta,\gamma}\frac{dx^\gamma}{d\tau}\xi^\alpha v^\beta + \Gamma^\mu_{\alpha\beta}\frac{d\xi^\alpha}{d\tau}v^\beta + \Gamma^\mu_{\alpha\beta}\xi^\alpha\frac{dv^\beta}{d\tau}, \tag{1.2.11}$$

Since each particle's worldline is a geodesic we also know that

$$\frac{dv^\beta}{d\tau} = \frac{d^2x^\beta}{d\tau^2} = -\Gamma^\beta_{\sigma\delta}v^\sigma v^\delta, \tag{1.2.12}$$

where again we have written $v^\beta = \frac{dx^\beta}{d\tau}$. Substituting equations (1.2.11) and (1.2.12) into (1.2.10) and permuting some repeated indices, we obtain

$$\frac{D^2\xi^\mu}{D\tau^2} = \frac{d^2\xi^\mu}{d\tau^2} + \Gamma^\mu_{\alpha\beta,\gamma}v^\gamma\xi^\alpha v^\beta + \Gamma^\mu_{\alpha\beta}\frac{d\xi^\alpha}{d\tau}v^\beta + \Gamma^\mu_{\sigma\delta}\frac{d\xi^\sigma}{d\tau}v^\delta - \left(\Gamma^\mu_{\beta\delta}\Gamma^\beta_{\alpha\sigma} - \Gamma^\mu_{\alpha\beta}\Gamma^\beta_{\alpha\delta}\right)v^\sigma v^\delta\xi^\alpha, \tag{1.2.13}$$

However we can now use the result we obtained in equation (1.2.6) i.e.

$$\frac{d^2\xi^\mu}{d\tau^2} = -\left(\Gamma^\mu_{\alpha\beta}v^\alpha\frac{d\xi^\beta}{d\tau} + \Gamma^\mu_{\alpha\beta}v^\beta\frac{d\xi^\alpha}{d\tau} + \Gamma^\mu_{\alpha\beta,\gamma}\xi^\gamma v^\alpha v^\beta\right) \tag{1.2.14}$$

so that finally we obtain the compact expression

$$\frac{D^2\xi^\mu}{D\tau^2} = R^\mu_{\alpha\beta\gamma}v^\alpha v^\beta\xi^\gamma \tag{1.2.15}$$

where

$$R^\mu_{\alpha\beta\gamma} = \Gamma^\sigma_{\alpha\gamma}\Gamma^\mu_{\sigma\beta} - \Gamma^\sigma_{\alpha\beta}\Gamma^\mu_{\sigma\gamma} + \Gamma^\mu_{\alpha\gamma,\beta} - \Gamma^\mu_{\alpha\beta,\gamma} \tag{1.2.16}$$

The (1, 3) tensor, R, in equations (1.2.13)_(1.2.16) is the Riemann_Christoffel tensor referred to at the beginning of this section. If spacetime is flat then

$$R^{\mu}_{\alpha\beta\gamma} = 0 \tag{1.2.17}$$

i.e. all components of the Riemann_Christoffel tensor are identically zero. We then see from equation (1.2.15) that the acceleration of the geodesic deviation is identically zero i.e. the separation between neighbouring geodesics remains constant. Conversely, however, if the space_time is curved then the geodesic separation changes along the worldline of neighbouring particles.

For a comparison of the relativistic and Newtonian equation for the tidal force, assume that the particle under consideration are moving slowly with

$$\frac{dx^{\alpha}}{d\tau} \simeq (1, 0, 0, 0) \tag{1.2.18}$$

Further more assume that ξ^0=0 ; this simply means that the particle acceleration are compared at equal times. Then equation (1.2.15) reduce to

$$\frac{d^2\xi^{\kappa}}{d\tau^2} = -R^{\kappa}_{0\iota 0}\xi^{\iota} \tag{1.2.19}$$

The tidal force is therefore

$$F^{\kappa}_{t} = -mR^{\kappa}_{0\iota 0}\xi^{\iota} \tag{1.2.20}$$

where m is the mass of the particle and ξ^{ι} its displacement from the origin. Note that this equation is valid only if the displacement and the velocity are small($\xi^{\iota}\to 0$, $\frac{d\xi^{\iota}}{d\tau}\to 0$). To establish that this equation for the tidal force is in agrement with the Newtonian expression(1.1.3). We must check that the old equation (1.1.3) and a new(1.2.16) definition of $R^{\kappa}_{0\iota 0}$ considered in weak static gravitational fields .In linear approximation, the two term quadratic in $\Gamma^{\alpha}_{\beta\mu}$ can be omitted from equation (1.2.16). Further more in this approximation

$$\Gamma^{\alpha}_{\beta\mu} = \frac{k}{2}\eta^{\alpha\delta}\left(h_{\delta\beta,\mu} + h_{\mu\delta,\beta} - h_{\beta\mu,\delta}\right), \tag{1.2.21}$$

This result in

$$R^{\alpha}_{\beta\mu\nu} \simeq -\frac{k}{2}\eta^{\alpha\delta}\Big(h_{\mu\delta,\beta,\nu} - h_{\beta\mu,\delta,\nu} - h_{\nu\delta,\beta,\mu} + h_{\beta\nu,\delta,\mu}\Big), \tag{1.2.22}$$

Therefore

$$R^{\kappa}_{0\iota 0} \simeq -\frac{k}{2}\Big(h_{\iota\kappa,0,0} - h_{0\iota,\kappa,0} - h_{0\kappa,0,\iota} + h_{00,\kappa,\iota}\Big), \tag{1.2.23}$$

In the Newtonian limit all the terms containing time derivative can be omitted and using

$$\frac{1}{2}kh_{00} = \Phi \tag{1.2.24}$$

We find

$$R^{\kappa}_{0\iota 0} = \frac{\partial^2\Phi}{\partial x^{\kappa}\partial x^{\iota}} \tag{1.2.25}$$

Which is in agrement with equation (1.1.3). The tidal force equation 1.2.19 can be used for measuring the component of $R^{\kappa}_{0\iota 0}$ of Riemann tensor, not that those measurement are performed locally. The Riemann tensor is therefore entirely determined by tidal force measurement. We might say that spacetime curvature and tidal forces represent the same physical entity, or to put it in Bondis words, Einsteins theory of gravitation has its physical and logical roots . . . in the existence of Newtonian tidal forces [1].

We will show that the tidal force satisfy

$$\frac{\partial F^{\kappa}_{t}}{\partial \xi^{\kappa}} = 0 \tag{1.2.26}$$

This means that the tidal force field can be represented graphically by field line .Of course, we already come across this condition in Newtonian theory but for the general proof we need to use the exact field equation. According to equation (1.2.11)

$$\frac{\partial F^{\kappa}_{t}}{\partial \xi^{\kappa}} = -mR^{\kappa}_{0\iota 0}\frac{\partial \xi^{\iota}}{\partial \xi^{\kappa}} = -mR^{\kappa}_{o\kappa o}, \tag{1.2.27}$$

Since $R^{\alpha}_{\beta\mu\nu}$ is antisymmetric in μ and ν we have $R^{0}_{000} = 0$,is therefore equivalent to

$$\frac{\partial F^{\kappa}_{t}}{\partial \xi^{\kappa}} = -mR^{\mu}_{o\mu o} = -mR_{00} \tag{1.2.28}$$

Where $R_{00} = R^{\mu}_{0\mu 0}$ is the component of the Ricci tenser. As we know Einstein's field equations in vaccum tell us that $R_{00} = 0$ and hence eq.(1.2.17) is valid as long as we remain out side of the mass distribution that generate the gravitational field.

1.3 Geodetic Precession

One of the characteristics of curved space is that parallel transport of a vector alters its direction, which suggests that we can probably detect the curvature of the space-time near the Earth by actually examining parallel transport. But to perform such an experiment, we must first devise some physical procedure for the parallel transport of a vector. From non gravitational physics we know that if a gyroscope is suspended in frictionless gimbals the result is a parallel transport of its spin direction. However from this we can not immediately draw the conclusion that in gravitational physics the transport of such gyroscope will also result in parallel transport of the direction of its spin. To find under what conditions transport of gyroscope result in Parallel transport, we start with equation of motion for the spin of a rigid body. According to Newton's theory a rigid body in a gravitational field is subject to a tidal torque given by equation (1.1.16) Which leads to a rate of change of spin given by[2]

$$\frac{dS^{\eta}}{d\tau} = \varepsilon^{n\kappa\iota} R^{\kappa}_{0\iota 0}\bigg(- I^{\iota\varepsilon} + \frac{1}{3}\delta^{\iota}_{s} I^{rr}\bigg), \tag{1.3.1}$$

Where n; k; l; s; r =1 ; 2 ; 3 . Here $R^{\kappa}_{0\iota 0}$ is the Riemann tensor evaluated in the rest frame of the gyroscope, the presence of which signifies that this particular equation of motion does not obey the principle of minimal coupling, and that the gyroscope spin transport does not imitate parallel transport and the quantity $\varepsilon^{\kappa\iota m}$ is defined by equation (1.1.17). For a spherical gyroscope we have that $I^{\iota s} \propto \delta^{\iota}_{s}$, then the tidal torque in the equation (1.1.16) becomes zero and the equation reads $\frac{ds^{n}}{dt} = 0$. I^{s}_{ι} is the moment of inertia tensor defined in the equation (1.1.5). This Newtonian equation remains in tact when we are in curved space_time, and in a reference frame that freely falls along a geodesic line. Thus the Newtonian time t must now interpreted as the proper time τ measured along the geodesic. In the freely falling reference frame the spin of the gyroscope remains constant in magnitude and direction, which means that it moves by parallel transport.

If now an extra non gravitational force acts on the gyroscope and as a result the gyroscope

moves into a world line that is different from a geodesic, then we can not simply introduce local geodesic coordinates at every point of this world line which makes the equation of motion for the spin $\frac{ds^n}{dt} \neq 0$. In flat space-time the precession of an accelerated gyroscope is called Thomas Precession. In a general coordinate system the spin vector S^μ in parallel transport obeys the equation:

$$\frac{dS^\mu}{d\tau} = -\Gamma^\mu_{\nu\lambda} S^\nu \frac{dx^\lambda}{d\tau} \tag{1.3.2}$$

where $\Gamma^\mu_{\nu\lambda}$ are the Christoffel symbols second kind, and S^μ are the spin vector components (here $\mu;\nu$; $\lambda = 0; 1; 2; 3$). From the above equation we can calculate how the spin of our gyroscope changes direction while the gyroscope moves along some free-fall trajectory. To be specific let us assume that the gyroscope in a circular orbit of radius r around the Earth. In real life somebody measures the change of the gyroscope spin relative to the fixed stars, which is also equivalent of finding this change with respect to a fixed coordinate system at infinity. We can use cartesian coordinates since they are more convenient in calculating this change of spin direction than polar coordinates. The reason for this is that in Cartesian coordinates any change of the spin can be directly related to the curvature of the space- time, where in polar coordinates there is a contribution from both coordinate curvature and curvature of the space_time. We will not therefore use the exact Schwarzschild solution but only the approximate solution in isotropic rectangular coordinates x, y, z

$$ds^2 \simeq \left(1 - \frac{2GM}{r}\right) dt^2 - \left(1 + \frac{2GM}{r}\right)^{-1} \left(dx^2 + dy^2 + dz^2\right) \tag{1.3.3}$$

Further assume that our gyroscope is in orbit around the Earth and let the orbit be located in the x-y plane as shown in Figure 1.3. For convenience we will evaluate equation (1.3.2) at one point of the orbit say, the point x = r, y = 0, z = 0. In a circular orbit all points are equivalent and if we know the rate of the spin change at one point we can calculate the rate of change of the spin at any point. For that let us write the line interval in the

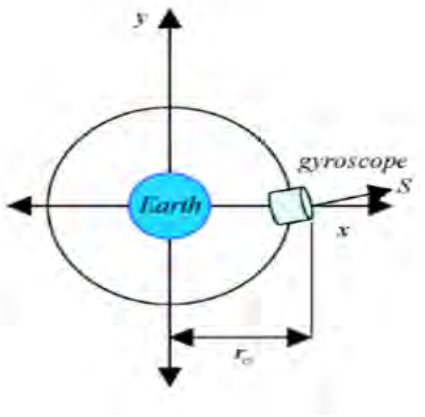

Figure 1.3: Gyroscope is in orbit around the Earth in x-y plane at one instant ,the one instance the gyroscope is at the point x = r, y = 0, z = 0

following way [9]:

$$ds^2 \simeq \left(1 - \frac{2GM}{r}\right) dt^2 - \left(1 + \frac{2GM}{r}\right)\left(dx^2 + dy^2 + dz^2\right) \tag{1.3.4}$$

which implies that:

$$g_{00} = \left(1 - \frac{2GM}{r}\right), \qquad g_{11} = g_{22} = g_{33} = \left(1 + \frac{2GM}{r}\right) \tag{1.3.5}$$

To evaluate the spatial components of the spin we will use equation (1.3.2), and the right hand symbols must be calculated. For that we need the four-velocity $v^\beta(v_t; v_x; v_y; v_z) =$ (1; 0; v; 0). We also need the S^0 component of the spin, and for that we note that in the rest frame of the gyroscope $S^0 = 0$ and v^β= (1; 0; 0; 0) and therefore $g_{\mu\nu}^{,}S^{,\nu}v^{,\nu}$=0, and also in our coordinate system we will also have that $g_{\mu\nu}S^\nu v^\nu = 0$, using the latter we have that:

$$S^0 = \frac{1}{g_{00}}\left(S^1 g_{11}\frac{dx^1}{d\tau} + S^2 g_{22}\frac{dx^2}{d\tau} + S^3 g_{33}\frac{dx^3}{d\tau}\right), \tag{1.3.6}$$

$$S^0 = \frac{1}{g_{00}}\left(S_x g_{11}\frac{dx}{d\tau} + S_y g_{22}\frac{dy}{d\tau} + S_z g_{33}\frac{dz}{d\tau}\right), \tag{1.3.7}$$

Substituting for the metric coefficients we obtain

$$S^0 = \left(\frac{1 + \frac{2GM}{r}}{1 - \frac{2GM}{r}}\right) v S_y \cong v S_y \tag{1.3.8}$$

Next letting μ= 1 and summing over $\nu = 0; 1; 2; 3$ the component of the spin equation becomes:

$$\frac{dS^1}{d\tau} = -\Gamma^1_{0\lambda} S^0 \upsilon^\lambda - \Gamma^1_{1\lambda} S^1 \upsilon^\lambda - \Gamma^1_{2\lambda} S^2 \upsilon^\lambda - \Gamma^1_{3\lambda} \upsilon^\lambda, \tag{1.3.9}$$

summing over $\lambda = 0; 1; 2; 3$ again we obtain:

$$\begin{aligned}\frac{dS^1}{d\tau} = &-\Gamma^1_{00} S^0 \upsilon^0 - \Gamma^1_{01} S^0 \upsilon^1 - \Gamma^1_{02} S^0 \upsilon^2 - \Gamma^1_{03} S^0 \upsilon^3 \\ &-\Gamma^1_{10} S^1 \upsilon^0 - \Gamma^1_{11} S^1 \upsilon^1 - \Gamma^1_{12} S^1 \upsilon^2 - \Gamma^1_{13} S^1 \upsilon^3 \\ &-\Gamma^1_{20} S^2 \upsilon^0 - \Gamma^1_{21} S^2 \upsilon^1 - \Gamma^1_{22} S^2 \upsilon^2 - \Gamma^1_{23} S^2 \upsilon^3 \\ &-\Gamma^1_{30} S^3 \upsilon^0 - \Gamma^1_{31} S^3 \upsilon^1 - \Gamma^1_{32} S^3 \upsilon^2 - \Gamma^1_{33} S^3 \upsilon^3,\end{aligned} \tag{1.3.10}$$

Next we will calculate the Christoffel symbols of the second kind for that we use:

$$\Gamma^\delta_{\mu\nu} = \frac{1}{2} g^{\delta\lambda} \left(\frac{\partial g_{\mu\delta}}{\partial x^\nu} + \frac{\partial g_{\nu\delta}}{\partial x^\mu} - \frac{\partial g_{\mu\nu}}{\partial x^\delta} \right), \tag{1.3.11}$$

Since $\Gamma^\delta_{\mu\nu}$= 0 if $\mu = \nu = \delta$ equation (1.3.10) further simplifies to

$$\begin{aligned}\frac{dS^1}{d\tau} = &-\Gamma^1_{00} S^0 \upsilon^0 - \Gamma^1_{01} S^0 \upsilon^1 - \Gamma^1_{02} S^0 \upsilon^2 - \Gamma^1_{03} S^0 \upsilon^3 \\ &-\Gamma^1_{10} S^1 \upsilon^0 - \Gamma^1_{11} S^1 \upsilon^1 - \Gamma^1_{12} S^1 \upsilon^2 - \Gamma^1_{13} S^1 \upsilon^3 \\ &-\Gamma^1_{20} S^2 \upsilon^0 - \Gamma^1_{21} S^2 \upsilon^1 - \Gamma^1_{22} S^2 \upsilon^2 - \Gamma^1_{23} S^2 \upsilon^3 \\ &-\Gamma^1_{30} S^3 \upsilon^0 - \Gamma^1_{31} S^3 \upsilon^1 - \Gamma^1_{32} S^3 \upsilon^2 - \Gamma^1_{33} S^3 \upsilon^3,\end{aligned} \tag{1.3.12}$$

The only non-zero Christoffel symbols calculated at $r = r_0$ are:

$$\begin{aligned}&\Gamma^1_{01} = \Gamma^1_{10} = -\frac{GM}{r_0^2}, \qquad \Gamma^1_{00} = -\frac{GM}{r_0^2}, \qquad \Gamma^1_{22} = -\frac{GM}{r_0^2} \\ &\Gamma^1_{21} = \Gamma^1_{12} = -\frac{GM}{r_0^2}, \qquad \Gamma^1_{33} = -\frac{GM}{r_0^2}, \qquad \Gamma^1_{13} = \Gamma^1_{31} = -\frac{GM}{r_0^2}\end{aligned} \tag{1.3.13}$$

Thus equation (1.3.12) further becomes:

$$\frac{dS_x}{d\tau} = -\Gamma^1_{00} S^0 - \Gamma^1_{22} S^2 \upsilon^2 \tag{1.3.14}$$

substituting we obtain:

$$\frac{dS_x}{d\tau} = -\frac{GM}{r_o^2} s_y \upsilon - \frac{GM}{r_o^2} s_y \upsilon \tag{1.3.15}$$

we can rewrite as follows:

$$\frac{dS_x}{d\tau} = -2\frac{GM}{r_o^2} s_y \upsilon \tag{1.3.16}$$

Similarly the equation for the S_y component of the spin becomes:

$$\frac{dS_y}{d\tau} = -\Gamma^2_{12} \upsilon S_x - \Gamma^2_{20} S_y - \Gamma^2_{22} S_y \upsilon - \Gamma^2_{32} S_y \upsilon, \tag{1.3.17}$$

which becomes:

$$\frac{dS_y}{d\tau} = -\frac{GM}{r_o^2} s_x \upsilon \tag{1.3.18}$$

Finally the equation for the S_z component becomes

$$\frac{dS_z}{d\tau} = 0 \tag{1.3.19}$$

Equations (1.3.16), (1.3.18), (1.3.19) are valid at the chosen x = r_0 , y = z = 0 point. These equations can also be written in a form that is valid at any point of the orbit, if we just recognize that all of them can be combined in the following single 3-D equation in the following way [7]:

$$\frac{dS}{d\tau} = -2\mathbf{v}.\mathbf{s}\nabla\Phi + \mathbf{v}\mathbf{s}.\nabla\Phi \tag{1.3.20}$$

where $\Phi = \frac{GM}{r_0}$ is the Newtonian potential. Since both the velocity $\mathbf{v}$ and the gradient $\nabla\Phi$ vary with position around the orbit the behavior of S given by equation (1.3.20) is rather complicated with small periodic oscillation in both the magnitude and the direction of S. However we are not interested in such periodic wobbles but only in the long-term secular change in S. We can calculate this secular change by taking the average of equation (1.3.20) over an orbit. For this purpose we express $\mathbf{v}$ and $\nabla\Phi$ as a function of time

$$\upsilon = -\hat{i}\ \upsilon\ sin(wt) + \hat{j}\ \upsilon\ cos(wt) \tag{1.3.21}$$

$$\nabla\Phi = -\hat{i}\frac{GM}{r_0^2} cos(wt) + \hat{j}\frac{GM}{r_0^2} sin(wt) \tag{1.3.22}$$

If we insert these expressions in the right side of equation (1.3.20) and average over one period of the orbit, we find

$$\left\langle \frac{dS}{d\tau} \right\rangle = \frac{3}{2}\frac{GM}{r_0^2}\upsilon\left(-\hat{i}s_y + \hat{j}s_x \right) \tag{1.3.23}$$

We can rewrite this result more neatly as follows

$$\left\langle \frac{dS}{d\tau} \right\rangle = \frac{3}{2}\frac{GM}{r_0^2}\left(\mathbf{r}\times\mathbf{v}\right)\times\mathbf{S} \tag{1.3.24}$$

From equation (1.3.24) we sea that on the average **S** presses about the axis of the orbit with an angular velocity

$$\Omega_G = \frac{3}{2}\frac{GM}{r_0^2}\mathbf{r}\times\mathbf{v}, \tag{1.3.25}$$

This is the geodetic precession or de sitter precession. For a gyroscope in orbit 650km above the Earth , we can write an expression for the geodetic precession equal to:

$$\frac{3}{2}\frac{GM}{r_0^3}\sqrt{\frac{GM}{r_0}} \simeq 6.6 \; arc\; sec\; per\; year, \tag{1.3.26}$$

1.4 Tidal Forces in a Schwarzschild Spacetime

The Schwarzschild solution is one of the best-known exact solutions of the Einstein's equations and was derived a few months after the theory was proposed. Consider, therefore, a spherical coordinate system (t, r, θ ,φ) in vacuum. Impose the constraints that the metric is spherically symmetric and static (i.e. none of the functions $g_{\mu\nu}$ depends on t, θ, φ) and that the space_time is asymptotically flat (i.e. $g_{\mu\nu} = 1$ for r $\to\infty$). Under these conditions, the solution to the Einstein equations has a line element

$$ds^2 = -dt^2\left(1 - \frac{2GM}{r}\right) + dr^2\left(1 - \frac{2GM}{r}\right)^{-1} + r^2\left(d\theta^2 + sin^2\theta d\varphi^2\right), \tag{1.4.1}$$

The space_time described by (1.4.1) is that of a Schwarzschild black hole, where M is the black-hole mass. Note that despite our intuition and the familiar concept of mass, the Schwarzschild metric is a solution of the Einstein's equations in vacuum, i.e.

$$R_{\mu\nu} = 0, \tag{1.4.2}$$

Indeed, the line element (1.4.1) is the only spherically symmetric and asymptotically flat solution that the equations admit (this is the thesis of Birkhoff's theorem). Because of this, the space_time exterior (i.e. for r$\geq R_*$, where R_* is the stellar radius) to a relativistic spherical (i.e. non rotating) star will also be given by the line element (1.4.1).

Let us consider what happens to an extended body located outside the black hole event horizon, is defined as the position at which the metric function $g_{tt} = 0$, i.e. at $r = 2M$. We will also assume that all the particles in the body move along geodesics and monitor how the separation between two nearby geodesics varies in time.

Obviously, Jacobivector fields provide the connection between the behavior of nearby particles and curvature, via the equation of geodesic deviation (Jacobi equation)

$$\frac{D^2\eta^\mu}{D\tau^2} = -R^\mu_{\alpha\delta\beta}\eta^\delta v^\alpha v^\beta \tag{1.4.3}$$

where v^μ are the components of the tangent vector to geodesic and η^μ are the components of the connecting vector between two neighboring geodesics.

The solution of the geodesic deviation equation (1.2.15) in the space_time (1.4.1) leads to the following expressions for the spatial components of η

$$\frac{D^2\eta^r}{D\tau^2} = \frac{2M}{r^3}\eta^r \tag{1.4.4}$$

This equation describe the tidal force in the radial direction .The deviation change is positive in this case it represent a radial tension or stretching effect

$$\frac{D^2\eta^\theta}{D\tau^2} = -\frac{M}{r^3}\eta^\theta \tag{1.4.5}$$

This equation describe a compression type pressure aligned along the transverse direction

$$\frac{D^2\eta^\phi}{D\tau^2} = -\frac{M}{r^3}\eta^\phi \tag{1.4.6}$$

This equation also describe a compression type pressure this time aligned along the transverse direction.

where the positive sign indicates a stretching and a negative one a compression in that

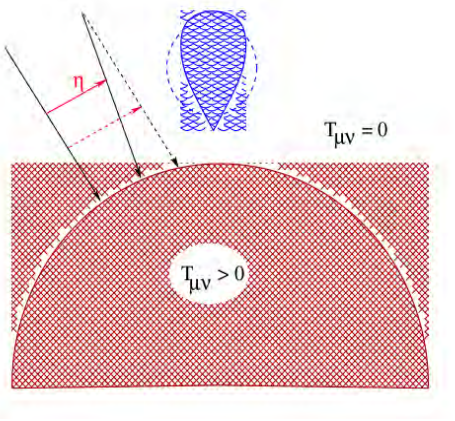

Figure 1.4: Schematic view of the geodesic deviation as well as of the deformation produced on a fluid body in the presence of a strong gravitational field. In the case considered here the source of the gravitational field is represented by a massive body (i.e. $T_{\mu\nu}>0$) but a qualitative similar scheme would be true also in the case of a black hole.

direction.

A schematic view of the geodesic deviation as well as of the deformation produced on a fluid body in the presence of a strong gravitational field, produced for instance by a compact star, are shown in Fig.1.4 for a plane at θ= const.

Two comments are worth making about expressions (1.4.4). Firstly the tidal deformation is finite at r = 2M and thus, depending on the black hole mass, the body may well preserve its shape when crossing the event horizon (This ceases to be true for r = 0 when the tidal stresses are divergent.). Secondly, the tidal fields at the horizon are larger for smaller black holes. This is simply because

$$\left|\frac{D^2\eta^a}{D\tau^2}\right| \sim \left|\frac{M}{r^3}\eta^a\right| \sim \left|\frac{1}{M^2}\eta^a\right|, \qquad at,\ r\sim M \tag{1.4.7}$$

For this reason, the tidal forces experienced in the vicinity of a supermassive black hole of, say, $10^8 M_\odot$ will be 16 orders of magnitude smaller than the corresponding ones near a stellar-mass black hole.

Chapter 2

Neutron Star

Neutron stars are extremely interesting objects, as they are the most known compact bodies without event horizons. They represent natural laboratories to test physics under extreme conditions, which are impossible to reproduce on Earth. Due to their compactness, NSs offer the unique chance to understand the properties of matter at supranuclear densities ($2.7\times10^{14} g/cm^3$). They are tiny (∼20 km diameter), HOT (>1,000,000 C), weigh between 1 and 3 solar masses, have strong magnetic fields (∼1 trillion gauss), and are rapid rotaters. Moreover, as previously noted, great interest behind this sources is justified by their GW emission.

2.1 Formation of Neutron Star

Neutron stars are comprised of an ultra-dense plasma of neutrons, with a superfluidlike core and solid crusty surface of metals and free electrons. Mass accretion onto a white dwarf may lead to collapse to a neutron star, and most are thought to be the collapsed cores of stars that have undergone a Type II supernova explosion.

2.2 Global Structure of Neutron Star

The structure of a neutron stars depends sensitively on its state of matter which is usually described as a pressure-density relation, P(ρ), namely the equation of state (EOS). The

adopted EOS has significant impact on global aspects of a neutron star (e.g. mass, radius). Stellar structure is determined by solving the equations of hydrostatic equilibrium. Owing to the strong gravity of neutron stars, general relativity has to be taken into account. In the time independent and spherically symmetric case, the metric at the stars interior is described by (with the convention G = c = 1):

$$ds^2 = -e^{2\Theta(r)}dt^2 + \frac{dr^2}{1-\frac{2m(r)}{r}} + r^2d\theta^2 + r^2sin^2\theta d\phi^2 \tag{2.2.1}$$

The metric function $e^{2\Theta(r)}$ and the global properties of the neutron star is then obtained by solving the following hydrostatic equation set:

$$\frac{dm}{dr} = 4\pi r^2\rho \tag{2.2.2}$$

$$\frac{dP}{dr} = -\frac{\rho m}{r^2}\left(1+\frac{P}{\rho}\right)\left(1+\frac{4\pi Pr^3}{m}\right)\left(1-\frac{2m}{r}\right)^{-1} \tag{2.2.3}$$

$$\frac{d\Theta}{dr} = -\frac{1}{\rho}\frac{dP}{dr}\left(1+\frac{P}{\rho}\right)^{-1} \tag{2.2.4}$$

Equation (2.2.3) usually called as Tolman-Oppenheimer-Volkoff (TOV) equation.

The boundary condition at r=0 is given by selecting a central density ρ_c and m(0)=0. Integrating the equations outward until P(r=R) = 0, then the mass and radius of the star is given by M = m(R) and R. One exact boundary condition is imposed on the metric function:

$$\Theta(R) = \frac{1}{2}ln\left(1-\frac{2M}{r}\right) \tag{2.2.5}$$

which ensure the function with match smoothly with the Schwarzschild metric that describe the spacetime at r>R.

The first neutron star structure was calculated by Tolman (1939) and Oppenheimer and Volkoff (1939).

2.3 Composition of Neutron Star

The structure of a neutron star can be divided into four major regions: the core, the crust, the envelope and the atmosphere. In this section, we are going to review the basic

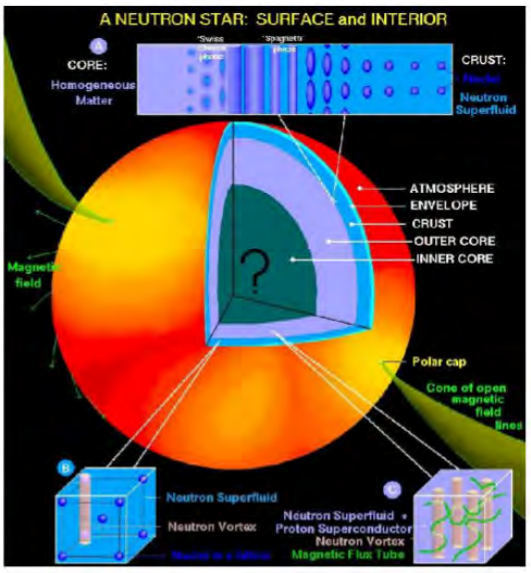

Figure 2.1: Illustration of the structure of the neutron star interior.

properties from the stellar surface to the inner core.

Envelope and Atmosphere

Although the atmosphere only has a thickness at the order of magnitude of a few centimeter, it can possibly alter the emergent photon spectrum from that of a perfect blackbody.

Crust

A solid crust , composed of two parts: (a) An outer crust whose density ranges from terrestrial densities to the neutron-drip density $\rho_{drip}\approx 4\times 10^{11} gcm^{-3}$: (b) An inner crust whose density ranges from the neutron-drip density $\rho_{drip}\approx 4\times 10^{11} gcm^{-3}$ to approximately the nuclear-matter density $\rho_{nm}\approx 2.8\times 1o^{14} gcm^{-3}$.

Core

A liquid core, in which the density steadily rises inward from ρ_{nm} to the central density ρ_c which is 4–7 times ρ_{nm} for modern EOS [9]. The core is thought to consist of the following parts: (a) An outer core, covering the density range from ρ_{nm} to $\sim 2\rho_{nm}$, is thought to be composed of uniform nuclear-matter consisting mostly of neutrons with protons and electrons in a small proportion. (b) An inner core, covering the density range from $\sim 2\rho_{nm}$ to ρ_c.

2.4 Rotation of Neutron Star

Neutron stars rotate extremely rapidly after their creation due to the conservation of angular momentum; like spinning ice skaters pulling in their arms, the slow rotation of the original stars core speeds up as it shrinks.Over time, neutron stars slow down because their rotating magnetic fields radiate energy. The rate at which a neutron star slows its rotation is usually constant and very small: the observed rates of decline are between 10^{-10} and 10^{-21} seconds for each rotation. Sometimes a neutron star will spin up or undergo a glitch, a sudden small increase of its rotation speed. Glitches are thought to be the effect of a starquake - as the rotation of the star slows down, the shape becomes more spherical. Due to the stiffness of the neutron crust, this happens as discrete events as the crust ruptures, similar to tectonic earthquakes. After the starquake, the star will have a smaller equatorial radius, and since angular momentum is conserved, rotational speed increases.

Recent work,however, suggests that a starquake would not release sufficient energy for a neutron star glitch; it has been suggested that glitches may instead be caused by transitions of vortices in the superfluid core of the star from one metastable energy state to a lower one.

Chapter 3

Superfluidity in Neutron Stars and Glitch Diagnostics

3.1 Superfluidity in Neutron Stars

Neutrons and protons in the nuclear matter found inside ordinary terrestrial nuclei are well-known to be superfluid, and the reason for this has been well- understood for a long time.The neutron-rich nuclei in the crust of a neutron star have the same property, and the dripped neutrons in the high-density inner crust are also superfluid. In the core, where the density is above the nuclear-matter density, and matter is predominantly neutrons with an appropriately small admixture of protons and electrons, both neutrons and protons are superfluid.

The usual, laboratory notion of a superfluid is one that flows without significant viscous dissipation, in contrast to what happens for ordinary fluids.The understanding of this physics in terms of correlations, i.e., in terms of the formation of pairs, in systems of fermions with attractive interactions has been one of the cornerstones of twentieth century physics, namely, the 1957 Bardeen-Cooper-Schriffer (BCS) theory of superconductivity.The basic idea is that, due to such pairing correlations, there is a major change in the low-energy spectrum of the system: a finite energy gap appears between its ground state and first excited states, and the system can undergo a phase transition to a superfluid below a critical temperature T_c.

3.1.1 Pairing

As pointed out in the original BCS work (1957a), pairing occurs essentially between fermion states near the Fermi surface. We can denote these fermion states as $|K\uparrow|$, $|-K\downarrow|$, and such pairs then form the ground state of the system. Because of pairing, it costs a finite amount of energy to excite a fermion from the ground state to the first excited state, the energy gap E_G , being given by the celebrated BCS equation:

$$E_G = kT_c = E_F exp\left[\frac{-1}{N(E_F)V}\right] \tag{3.1.1}$$

Here, E_F is the Fermi energy, N(E_F) is the density of states at the Fermi surface, and V is the effective interaction in the many-fermion system under study.

The formation of Cooper pairs in superfluids is an excellent example of the quantum-mechanical phenomenon of condensation: we can characterize condensation as macroscopic occupation of a single quantum state. What does this mean? In a superfluid, for example, the wave function of the condensate has the form $\Psi(R)\sim|\Psi(R)exp[i\theta(R)]|$, i.e., it is coherent in the phase θ(R) over the whole fluid.

3.1.2 Rotating Superfluids and Quantized Vortices

What happens when superfluids rotate? The answer to this question, which is at the heart of much of the rotational dynamics of neutron stars, had been known for a long time before the era of pulsars, from studies of rotating superfluid **He**$\_II$. From elementary quantum mechanics, the velocity $\mathbf{v}_s$ of a superfluid is given in terms of the (coherent) condensate phase θ introduced above by the expression

$$\mathbf{v}_s = \frac{\hbar}{2m_n}\nabla\theta \tag{3.1.2}$$

where $2m_n$ is the mass of a neutron pair. Since v_s is the gradient of a scalar, we get the immediate result that the flow of a superfluid is irrotational, i.e.,

$$\nabla\times\mathbf{v}_s = 0 \tag{3.1.3}$$

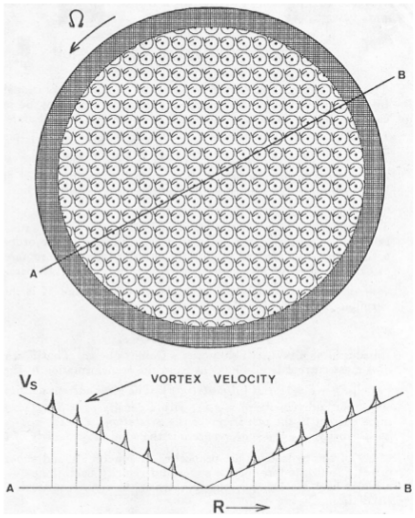

Figure 3.1: Vortex lines in a rotating superfluid.

except possibly at an isolated set of singularities [12]. These are actually line singularities, i.e., vortex lines.

The way a rotating superfluid carries angular momentum is, then, by forming these vortex lines, as shown in Fig. 3.1, and the strength of such a vortex is measured by the circulation or vorticity around it, defined and evaluated as follows, using Eq. (3.1.2):

$$k \equiv \oint \mathbf{v}_s . d\mathbf{l} = \frac{\hbar}{2m_n} \Delta\theta = n \frac{h}{2m_n}, \tag{3.1.4}$$

n being an integer. The wave function Ψ is assumed to be single-valued, so that its phase θ must change by an integral multiple n of 2π in going around the line. Thus, the vorticity is quantized in units of $\frac{h}{2m_n}$. In other words, quantized vortices must be present in rotating superfluids: this was pointed out long ago by Onsager (1949) and Feynman (1955), so that such vortices are sometimes called Onsager-Feynman vortices[14]. It is now easy to calculate the superfluid velocity v_s at a distance r from the vortex line, since $\oint \mathbf{v}_s . d\mathbf{l} = 2\pi r v_s$ because of cylindrical symmetry around this line. The result is:

$$v_s = \frac{n\hbar}{2m_n r} \tag{3.1.5}$$

The energy per particle of a vortex is given, to a first approximation, by the kinetic energy of the fluids rotation:

$$\varepsilon_{vort} = \frac{1}{N_n}\int \frac{1}{2} m_n \upsilon_s^2 n_n d^3 r \tag{3.1.6}$$

where n_n is the number density of neutrons, and N_n is the total number of neutrons present in the system [6]. The above integral extends over the entire rotating system, except very close to the center of the vortex, where the condensate wave function Ψ goes to zero, the phase coherence characteristic of superfluids is lost, and matter becomes normal. The radial extent of this normal vortex core is of the order of the coherence length d in the neutron superfluid, which can be roughly defined as that distance from the center of the vortex at which the kinetic energy density $(\frac{1}{2})m_n\upsilon_s^2 n_n$ of the superfluid equals the condensation energy density, the latter being given by the BCS theory. An approximate expression for the coherence length is:

$$d \cong \frac{\hbar^2 k_F^{(n)}}{\pi E_G m_n} \tag{3.1.7}$$

where E_G is the gap energy, as before, and k_F is the Fermi wave-number of the neutrons. For typical values $E_G \sim$1MeV (see above), and $k_F^{(n)} \sim 1 fm^{-1}$, we get $\varsigma \sim$10fm, setting the scale size of the vortex core. An alternative, useful form for ς given by Pines (1971)[15] is:

$$d = \frac{2}{\pi k_F^{(n)}}\left[\frac{E_F^{(n)}}{E_G}\right] \tag{3.1.8}$$

where $E_F^{(n)} \equiv 2\hbar^2\left(k_F^{(n)}\right)^2/2m_n$ is the Fermi energy of the neutrons[9].

Suppose we have neutron superfluid in a cylinder of radius R, and we make the cylinder rotate, starting from rest.Note first that, if the vortex line is along the axis of the cylinder, each neutron-pair has an angular momentum $2m_n\upsilon_s r = n\hbar$, with the aid of Eq. (3.1.5), so that each neutron has an angular momentum L = $\frac{n\hbar}{2}$. Similarly, each neutron has a rotational energy ε_{vort} given by Eq. (3.1.6), which, using Eq. (3.1.5) again,gives us

$$\varepsilon_{vort} = \frac{n^2\hbar^2}{4m_n R^2}\int_d^R \frac{dr}{r} = \frac{\hbar\Omega_{cl}}{2}n^2 \tag{3.1.9}$$

where $\Omega_{cl} \equiv (\hbar/2m_nR^2)ln(R/d)$ is a lower critical angular velocity, whose physical significance we shall now see. Suppose that we are making the container rotate at this moment with an angular velocity Ω. The equilibrium configuration is obtained by minimizing the free energy ε_{vort}-ΩL. Thus, we can readily show from the above expressions for energy and angular momentum per particle that, when $\Omega < \Omega_{cl}$, the least value of the above quantity is obtained for n = 0, i.e., no vortices present in the superfluid at all. This, then, is the situation below the lower critical angular velocity Ω_{cl}: the container rotates but the superfluid sits still [12]. The relevance to neutron stars must be evident by now: the container mimics the solid crust of the star, with R $\sim$10km. It is then clear that, with $d \sim 10$ fm as given above, $\Omega_{cl} \sim 10^{-14} s^{-1}$, i.e., a negligibly slow speed compared to the values $\Omega \geq 10^{-3} s^{-1}$ for the slowest-rotating neutron stars known. As Ω exceeds Ω_{cl}, a single quantized vortex appears first, then more and more as Ω increases. When $\Omega \gg \Omega_{cl}$ and the spacing between the vortices becomes $\ll$ R, as shown in Fig. 3.1, the flow pattern looks on a macroscopic scale like a uniform rotation, characterized by a density of vortices per unit area n_v , which is easily calculable in terms of the (uniform) angular velocity Ω and the vortex quantum $h/2m_n$. We write the circulation integral, $\int \mathbf{v}_s.d\mathbf{l}$, in two ways: (a) as $2\pi r\bar{v}_s$, in terms of the mean flow velocity $\bar{v}_s$ at a radius r, and (b) as $(n_v \pi r^2).(h/2m_n)$, since the first bracket gives the total number of vortices within a radius r, and the second, the quantum of circulation. Equating the two, we readily get $\bar{v}_s = (hn_v/4m_n)r$: this shows that the flow is a uniform rotation, $\bar{v}_s = \Omega r$, with an angular velocity $\Omega = (hn_v/4m_n)$. We thus arrive at the Onsager-Feynman expression for the areal density of vortices:

$$n_v = \frac{4m_n\Omega}{h} = \frac{2\Omega}{(h/2m_n)} \tag{3.1.10}$$

From elementary hydrodynamics, the circulation per unit area, $\nabla \times \mathbf{v}_s$, is just $2\Omega\hat{z}$ for a uniform rotation about the z-axis, as we can easily show by substituting $\mathbf{v}_s = \Omega\hat{z} \times \mathbf{r}$ in the above curl expression. The number of vortices per unit area must, therefore, be this amount of circulation, 2Ω, divided by the quantum of circulation given above.

Consider, finally, what happens at still faster rotation. When the vortex spacing approaches the coherence length d, so that vortex cores overlap, superfluidity ceases, as must be clear from the earlier observation that the condensate wave function vanishes within vortex cores. From the expressions given above, we can immediately show that this happens above an upper critical angular velocity $\Omega_{cu} \sim (\hbar/2m_n d^2) \sim 10^{20} s^{-1}$. Again, this is enormously large compared to the values $\Omega \leq 10^3 s^{-1}$ for the fastest-rotating millisecond pulsars known, and the limit of stability for rotating neutron stars is only about an order of magnitude higher than the above highest value seen in millisecond pulsars. Thus, pulsars always sit very safely between Ω_{cl} and Ω_{cu} [12], far away from either limit.

3.2 Post-Glitch Relaxation:Two-Component Theory

The long, macroscopic relaxation times ($\sim$tens to hundreds of days;) of the glitches made it clear from the beginning that superfluids were very likely involved in the process, since coupling through microscopic processes involving normal matter would be extremely tight, leading to time scales $\sim$seconds. Accordingly, a phenomenological, two- component theory of post-glitch relaxation was proposed in 1969 by Baym et al., in which a container or c-component rotated at a slightly lower angular velocity from the superfluid or s-component. The container component was actually the solid crust, plus any other (charged) component that was tightly coupled to the crust. The superfluid component was actually the neutron superfluid in the core of the neutron star, loosely coupled to the container. The two components were coupled by a mutual friction between them, with a long relaxation time τ of the order of magnitude given above, so that the coupling was described by a term $\propto (\Omega_s - \Omega_c)/\tau$ in the equations of rotational dynamics. The glitch was, of course,described in this theory as a starquake in the crust, as was customary at the time. Post-glitch relaxation then readily emerged from the theory as an exponential healing of a fraction Q of the glitch $\Delta\Omega$ on a time scale $\sim\tau$[9].

The microscopic process underlying such long relaxation times as above was believed in

the 1970s to be the scattering of electrons by the normal cores of the vortex lines in the neutron superfluid. In the early 1980s, however, re-investigations of this scattering process established that the dominant mechanism was, in fact, the scattering of electrons by the inhomogeneous magnetization surrounding vortex lines [16], and the timescale was far shorter than imagined before. This magnetization, which is typically $\sim 10^{15}$ G, arises from the current of super- conducting protons entrained by the superfluid neutron currents circulating around the vortex lines, and the timescale for the relaxation of the relative velocity between an electron and a vortex line is roughly $\tau_v \sim \Omega_2^{-1}$second. Here, Ω_2 is the pulsars angular velocity in units of 10^2 $rads^{-1}$. The corresponding dynamical coupling time τ_d between the crust and the superfluid neutron core is given roughly by $\tau_d \sim (20\_600)\tau_v \sim (1\_10)\Omega_2^{-1}$ minutes, i.e., essentially instantaneous compared to the observed relaxation times given above.

Thus, the original two-component theory also became untenable at about the same time as the starquake model did. It is interesting, however, that a later incarnation of the theory came into vogue in the 1980s when the next successful model of the glitches was proposed, and post-glitch relaxation needed to be explained from an altogether different point of view.

3.3 Glitches: Vortex Pinning

Following the realization that starquakes were untenable as a unified model of the glitch phenomenon, a novel mechanism involving the rotating neutron superfluid in a neutron star was suggested in the early 1980s and thoroughly studied subsequently.In an excellent 1971 review of the essential condensed-matter physics of neutron stars, Pines considered the possibility that the above quantized vortices in the superfluid dripped neutrons in the inner crust of the neutron star could be pinned to the lattice of the heavy, neutron-rich nuclei which exists there. Pinning means, as the word suggests, that the normal core regions of the vortex lines would prefer to pass through the positions of the crustal nuclei

on the lattice sites, and would stay fixed in this manner until a stronger force could unpin them from these sites. Although Pines already suggested in his original (1971) work that vortex pinning could be an important question in sorting out the response of the neutron system to sudden changes in crustal motion, Anderson and Itoh briefly reconsidered the idea in 1975, making the pioneering connection between sudden vortex unpinning and pulsar glitches, and stating that this idea explained the observations at least equally well (compared with the starquake scenario, which was still the standard model at the time). It is, in fact, instructive to compare the orders of magnitude of several length scales involved in the problem. First, there is the spacing between vortex lines, $r_v \sim 10^{-2}\sqrt{p(s)}$cm, which is enormous compared to all other lengthscales of the problem [15], and so irrelevant for the pinning criterion. Then, there is the coherence length d for dripped neutrons discussed above. Note that $d \leq 1$fm near the outer edge of the inner crust and that $d \sim 40$fm near the inner edge of the inner crust. Next, there is the lattice spacing b, the lattice spacing is b$\sim 60(A^{1/3}/5)$fm near the outer edge of the inner crust, and b$\sim 10(A^{1/3}/5)$fm near the inner edge. Note that, for the equilibrium nuclei in the inner crust, $A^{1/3}$ rises from $\sim$5 near the outer edge to $\sim$6_7 near the inner. Finally, there is the size of the nuclei at the lattice sites, $r_N \approx r_0 A^{1/3} \sim 6(A^{1/3}/5)$fm.

where A is the mass number of the equilibrum nuclides.

For exploring the pinning criterion, we thus need only consider the relative values of d, b, and r_N. Pines (1971) originally considered the ratio d/r_N, which is interesting for other considerations, but it became clear subsequently that d/b was the ratio crucial to geometrical criterion for pinning. Since

$$\frac{d}{b} \sim 7\left(\frac{E_G}{1MeV}\right)^{-1}\left(\frac{A^{2/3}}{5}\right)^{-1}\left(\frac{\rho}{\rho_{nm}}\right)^{2/3}\left(\frac{\rho_{dn}}{\rho-\rho_{dn}}\right) \tag{3.3.1}$$

we see that $d/b \sim 10^{-2}$ near the outer edge of the inner crust, and $d/b \sim 7$ near the inner edge. Thus, except in the innermost parts of the inner crust, $d/b \leq 1$, so that pinning to the lattice sites is a geometrically valid concept.

3.3.1 The Pinning Force

How do we calculate the pinning force and energy? The latter is calculated by a method which follows straight from the qualitative idea of pinning, namely, that pinning occurs when the energy that obtains if the vortex line passes through a nucleus is less than that which obtains if it threads through the intersterial region between nuclei: the pinning energy is simply the difference between the two. Neutrons inside the nuclei are superfluid, as are the dripped neutrons outside the nuclei. So, it is a matter of calculating the energy difference between creating a vortex core in the outer, dripped-neutron superfluid and creating one in the inner, nuclear superfluid. Then the pinning energy per unit volume is $(n_n\epsilon)_{out} - (n_n\epsilon)_{in}$, where n_n is the number density of superfluid neutrons.

The question is: what is ϵ? This energy, which is of basic importance in the physics of superfluid vortices, is given in terms of the gap energy E_G of the superfluid and the Fermi energy E_F of the fermions constituting the superfluid by $\epsilon \sim E_G^2/E_F$.

The pinning energy per nucleus E_p can now be written down in the form [16,17]:

$$E_p = \frac{3}{8}\left[\left(n_n \frac{E_{G(n)}^2}{E_F^{(n)}}\right)_{out} - \left(n_n \frac{E_{G(n)}^2}{E_F^{(n)}}\right)_{in}\right]V. \tag{3.3.2}$$

Here, the label (n) denotes neutrons, as before, and V is the overlap volume between the vortex core and the nucleus, Which is of the order of the nuclear volume $(4\pi/3)r_N^3$.

The pinning force F_p is obtained by dividing E_p by the length scale of the interaction between the vortex core and the nucleus, for which we can adopt the larger of the two lengths d and r_N [17], which, in view of the above discussions, is just d over essentially all of the region where effective pinning occurs. So, $F_p \approx E_p/d$ is a very good estimate. Finally, the pinning force f_p per unit length of the vortex line is given by $f_p = F_p/a$, where a is the spacing between successive pinning centers along the vortex line.

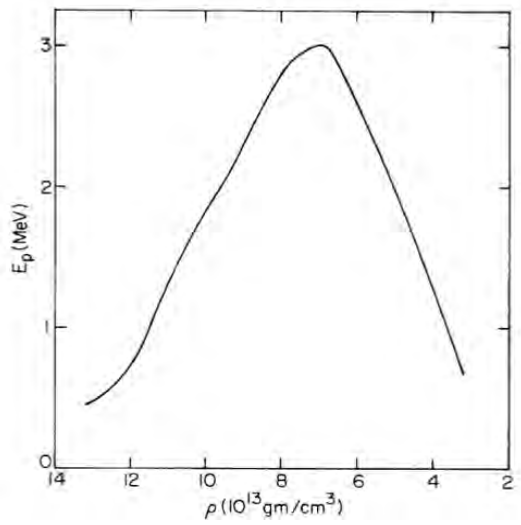

Figure 3.2: Pinning energy E_p per nucleus vs density in neutron-star crusts.

3.3.2 Strong and Weak Pinning

If the vortex lines were oriented exactly along one of the axes of the nuclear lattice, the spacing a between successive pinning centers would equal the lattice spacing b for a simple cubic lattice. This would lead to the largest possible value of f_p, i.e., optimal pinning. But this would happen only if the direction of the angular velocity Ω of the star, which is the direction of the vortex lines, coincided with that of one of the lattice axes, which will not be the case, in general. This is so because the conditions under which the crust solidified and the lattice froze had basically nothing to do with stellar rotation.The question is, what would optimize pinning under such conditions? The answer introduces us to the idea of strong pinning.

Imagine that the pinning force is so strong that it can displace the nuclei from their equilibrium lattice sites by amounts sufficient to arrange them along the vortex line. This is optimal indeed, since the spacing a between pinning centers along a vortex line will then be $\sim$ a few times the lattice spacing b [7]. The quantitative criterion for this strong pinning follows directly from its definition: the pinning force F_p must exceed the lattice displacement force F_L. Where, $F_L \sim [(\partial/\partial r)(Z^2e^2/r^2)]_{r=b}d \sim (Z^2e^2/b^3)d \sim (w_c/d)(d/b)^2$.

Here, $w_c \sim Z^2e^2/r_c \sim Z^2e^2/b$ is the Coulomb energy of a Wigner-Seitz cell. Hence, the strong-pinning condition, $F_p > F_L$, reduces to the condition $E_p > E_{crit}$ on the pinning energy, where the critical energy is $E_{crit} \equiv w_c(d/b)^2 \sim 1\_2MeV$ in the pinning region.

As we go inward through the pinning region, the density rises, and so does E_{crit} , since it scales as d^2/b^3 , and d increases and b decreases with increasing density. On the other hand, E_p passes through a maximum and falls with rising density, as shown above. Hence, above a critical density $\rho_{crit} \approx \rho_{nm}/3$, the strong-pinning condition is no longer valid, and we reach the re'gime of weak pinning, where $F_p < F_L$. What happens then? We might think at first that the vortex line would then bend as necessary to optimize pinning, since the pinning force is no longer strong enough to displace nuclei for this purpose. What is believed to happen instead is that the lattice does deform, but now more smoothly on a length scale a, rather in a wave- like fashion, along the vortex line [7].

We can estimate a in this situation by equating the orders of magnitude of the pinning and lattice-distortion energies, which must be valid at equilibrium. Per pinning site, the former energy is just E_p . To estimate the latter, note that a wave-like distortion of wavelength a and amplitude d leads to a relative displacement $\sim d/a$ in the lattice, and so to a lattice-distortion energy $\sim w_c(d/a)$ per pinning site. Equating these and using the expression for the critical pinning energy E_{crit}, we obtain

$$\frac{a}{b} \sim \frac{E_{crit}}{E_p}\frac{b}{d}, \tag{3.3.3}$$

which manifestly shows that a$\gtrsim$b, as it must be, since $E_p < E_{crit}$ and $d < b$ in this regime. Finally, the average spacing between pinning sites along the vortex line is given by:

$$a \approx \frac{b^3}{\pi d^2} \sim \frac{b^3}{d^2} \tag{3.3.4}$$

3.3.3 The Magnus Force

We now describe how the above phenomenon of pinning is relevant to glitches. A vortex line would tend to move with the ambient superfluid, unless there is some force in the

system which acts to prevent this. Now, the ambient superfluid moves with an angular velocity Ω_s which is determined by the areal density of vortices according to Eqn. (3.1.10). However, the vortex lines pinned to the crustal nuclei move with the solid crust, which generally moves at a lower angular velocity Ω_c . This is so because the electromagnetic torques which slow down a rotation-powered pulsar act directly only on the crust, and not on the superfluid of dripped neutrons in it. Thus, it is Ω_c that is to be identified with the observed angular velocity of the star, since pulsar emission processes are believed to be related to the external surface of the solid crust, and the magnetic field threading through it. Ω_s always lags behind it.

Because of this difference of velocities, $\delta\mathbf{v} = r(\Omega_s - \Omega_c)\hat{\phi}$, between a vortex line and its ambient superfluid, the former is acted upon by a force which is called the Magnus force, and which would neutralize the above velocity difference. Here, the angular velocities are oriented along the z-axis, and ϕ is the azimuthal angle around this axis. How the Magnus force would do this becomes clear when we write its value f_M per unit length of the vortex line as:

$$f_M = -\rho(k\hat{z}) \times \delta v. \tag{3.3.5}$$

Here,$k = h/2m_n$is the vorticity quantum , so that $\hat{z}$ is the vorticity vector. From Eq. (3.3.5) and the above expression for δv, it is clear that the Magnus force acts in the radially outward direction, i.e., it tends to push the vortex lines outward, so as to transfer some of the angular momentum of the superfluid to the crust, thus spinning up the latter, and reducing the above difference of velocities.

The Magnus force is counteracted by the pinning force f_p , which acts in a radially inward direction, and keeps the vortex lines pinned to the nuclei, as long as the pinning force exceeds the Magnus force, $f_p > f_M$. Given a strength of the pinning force, the difference in angular velocities, $\delta\Omega \equiv \Omega_s - \Omega_c$, thus builds up as the crust spins down, until it becomes so large that $f_p = f_M$. At this point, the vortex lines unpin from the nuclei suddenly, moving outward and transferring their angular momentum to the crust in a

catastrophic manner, thus causing a sudden speed-up of the crust, i.e., a glitch. The critical angular-velocity difference, $\delta\Omega_{crit}$, at which this happens is readily obtained by inserting the expressions for f_p and f_M given earlier into the above condition of their equality at the unpinning point:

$$\delta\Omega = \frac{E_p}{dar\rho k} \tag{3.3.6}$$

We show the variation of $\delta\Omega_{crit}$ with density from an early calculation [5], using the original Hoffberg et al. (1970) results for the gap energy, and variations thereof. Clearly, the value of the critical angular-velocity difference depends sensitively on the gap energy.

3.4 Post-Glitch Relaxation: Vortex Creep

Between glitches, the vortex lines are believed to undergo a slow, thermally activated process called vortex creep, which is a quantum tunneling between adjacent sites which are geometrically suitable for pinning. In this picture, the creep process approaches a steady state when left to itself, a glitch perturbs it away from this steady state, and the post-glitch relaxation is a process of recoupling the creep to another steady state. A simple, potential- field description in terms of the pinning-energy profile[18], clearly explains the essential physics of vortex creep, and we recount it here in brief.

Consider, schematically, the potential seen by a vortex line in a lattice in the pinning regime, i.e., where pinning is energetically favorable. The nuclei represent sites of lower energy potential wells and the spaces between them have higher energies, i.e., barriers between these wells, the difference between these being $\sim E_p$. E_p is the order of magnitude of the amplitude of variation this quasi-periodic potential, whose periodicity in space is ∼a, the average distance between pinning centers.Now consider what happens because of the angular-velocity difference $\delta\Omega$ between the superfluid and the pinned vortex. The Magnus force per unit length $f_M = \rho r\delta\Omega\hat{r}$ tends to push the vortex lines outward, as we argued above. We can now cast this into a potential description by first noting that the force per pinning site is $F_M \approx f_M a$, and then that the energy difference corresponding to

this force would be $\Delta E_p \sim F_M d$. Thus, a site at a distance r from the rotation axis will have an energy higher than one at a distance $\sim$ a further from the axis by an amount

$$\Delta E_p \sim dar\rho k\delta\Omega = E_p \frac{\delta\Omega}{\delta\Omega_{crit}}, \tag{3.4.1}$$

where we have used Eq. (3.3.6) to obtain the last expression. The profile, while still quasiperiodic with a spacing $\sim$ a and an amplitude $\sim E_p$, now has an overall downward slope in the radially outward direction. This favors thermally- activated barrier penetration in a radially outward direction over that in an inward direction, and so produces an overall outward drift of the vortex lines. This, precisely, is the vortex creep.

We can calculate the radial creep velocity v_r from barrier-penetration considerations in a straightforward manner [16]. For motion in an outward direction, the energy barrier is lowered to $E_{out} = E_p - \Delta E_p = E_p[1 - (\delta\Omega/\delta\Omega_{crit})]$, while for motion in an inward direction, it is raised to $E_{in} = E_p + \Delta E_p = E_p[1 + (\delta\Omega/\delta\Omega_{crit})]$. Hence the overall creep velocity in the radially outward direction is:

$$v_r = v_o \left[exp\left(-\frac{E_{out}}{kT} \right) - exp\left(-\frac{E_{in}}{kT} \right) \right] \tag{3.4.2}$$

where v_0 is the velocity scale for microscopic motion of the vortex lines between pinning sites. A form of Eq. (3.4.2) that we shall find of much practical use below is

$$\begin{aligned} v_r &= 2v_o \; exp\left[\left(-\frac{E_p}{KT} \right) sinh\left(\frac{\delta\Omega}{\langle\delta\Omega\rangle} \right) \right] \\ &\approx v_o \; exp\left(-\frac{E_p}{KT} \right) exp\left(\frac{\delta\Omega}{\langle\delta\Omega\rangle} \right). \end{aligned} \tag{3.4.3}$$

Here, we have defined a reference value of the angular-velocity difference, or lag, $\delta\Omega$, by the relation $\langle\delta\Omega\rangle \equiv (kT/E_p)\delta\Omega_{crit}$. The second, approximate form of Eq. (3.4.3) applies when $\delta\Omega$ is close to $\delta\Omega_{crit}$, since $E_p \sim 1MeV$, and $kT \lesssim 1keV$.

3.4.1 Rotational Dynamics: Steady State

An excellent approach to the rotational dynamics of the star according to the above scenario of vortex pinning, catastrophic unpinning, and gradual creep is in terms of a

two-component theory, which we now describe. The first component is again the container , i.e., those parts of the star which rotate quite rigidly together as one body, and are acted upon by directly by the external torque N_{ext} . The second component is the superfluid, which rotates with an angular velocity different from that of the above c-component. This s-component now actually consists of the crustal superfluid alone. Note that, although the s-component contains only $\sim 10^{-2}$ of the total moment of inertia of the star, it is thus dynamically crucial in this scenario for explaining glitches, post-glitch relaxation, and associated phenomena [16].The coupling between the two components is now completely different from the frictional coupling postulated in the two-component theory of the starquake era.

The rotation of the c-component is described quantitatively by:

$$I_c\dot{\Omega}_c = N_{ext} + N_{int}, \qquad N_{int} \equiv -\int dI_s\dot{\Omega}_s, \tag{3.4.4}$$

where the internal torque N_{int} arises from the s-component, the integration extending over all possible parts of that component. From observation, we know that $N_{int} \sim 10^{-2} N_{ext}$. On the other hand, the rotation of the s-component is obtained by combining the law of vortex conservation,

$$\frac{\partial n_v}{\partial t} + \nabla.(n_v \upsilon_r \hat{r}) = 0 \tag{3.4.5}$$

with a generalization of Eq. (3.1.4) to a situation where there can be differential rotation in the superfluid, so that both Ω_s and n_v can be functions of the radial co-ordinate r:

$$\oint \mathbf{v}_s.d\mathbf{l} = 2\pi\Omega_s(r)r^2 = k\int_0^r 2\pi r n_v(r)dr \tag{3.4.6}$$

Here, n_v is, of course, the areal density of vortices, and $k \equiv h/2m_n$ is vorticity quantum. The differential form of Eq. (3.4.6), which reads $n_v(r) = 2\Omega_s(r) + r(\partial\Omega_s/\partial r)$, can be combined with Eq. (3.4.5) to yield the required quantitative description of the rotation of the s-component:

$$\frac{\partial\Omega_s}{\partial t} = -\frac{kn_v\upsilon_r}{r} = -\frac{2\Omega_s(1+\epsilon)\upsilon_r}{r} \tag{3.4.7}$$

Here, $\epsilon(r)\equiv(r/2\Omega_s)(\partial\Omega_s/\partial r)$ is the differential-rotation parameter of the superfluid. For the radial creep velocity of vortices, we use Eq. (3.4.2), and this completes the description. We now summarize some essential features of the rotational behavior described by the solutions of the above equations: First, this description indicates the existence of a steady-state solution, corresponding to a constant asymptotic value of the lag $\delta\Omega_\infty$. It is easily obtained from the requirement that, in this steady state, the s- and c-components spin down at the same rate, $\partial\Omega_s/\partial t = \dot{\Omega}_c = \dot{\Omega}_\infty$, say, so that the lag stays constant at $\delta\Omega_\infty$. With the aid of Eq. (3.4.4), we see that the steady-state spin-down rate is given by $\dot{\Omega}_\infty = \dot{\Omega}_c = N_{ext}/I$, where $I\equiv I_c + \int dI_s$ is total moment of inertia of the star. Further, the steady-state creep velocity is obtained from Eq. (3.4.7), and expressed as:

$$\upsilon_\infty = \frac{|\dot{\Omega}_\infty| r}{2\Omega_s(1+\epsilon)} \approx \frac{r}{2t_s} \tag{3.4.8}$$

in terms of an (observable) spin-down timescale of the star, $t_s\equiv\Omega_c/|\dot{\Omega}_\infty|$, which can be closely approximated by $t_s\approx\Omega_s/|\dot{\Omega}_\infty|$, since $\delta\Omega\ll\Omega_s$, we described above. In obtaining the last approximation in Eq. (3.4.8), we have neglected the superfluids differential-rotation parameter , it mimics such rotation very closely by creating a dense array of quantized vortices.

A simple description of the above steady state is thus that (a) the vortices creep over a distance comparable to the stellar radius in a spin-down time t_s , such that (b) the crustal superfluids angular velocity just keeps up with the change in the angular velocity of the crust (and the core tightly coupled to it) produced by the external spin-down torque on the pulsar. It is now easy to see that the steady-state $\delta\Omega_\infty$ must be close to $\delta\Omega_{crit}$, and so would the actual $\delta\Omega$ for expected rotational states of the pulsar, as stated earlier. We do this by applying the approximate form of Eq. (3.4.3) to steady-state creep, which yields

$$1 - \frac{\delta\Omega_\infty}{\delta\Omega_{crit}} = \frac{kT}{E_p} ln\left(\frac{2t_s\upsilon_0}{r}\right) \tag{3.4.9}$$

with the aid of Eq. (3.4.8). Now, on the right-hand side of Eq. (3.4.9), the logarithmic factor is $\sim$10_30, but $kT/E_p<10^{-3}$, so that the right-hand side is $\ll$1 quite generally,

and consequently $\delta\Omega_\infty$ is always close to $\delta\Omega_{crit}$. Glitches occur preferentially, of course, in those regions of the crust where $\delta\Omega_\infty$ is closest to $\delta\Omega_{crit}$.

3.4.2 Approach to Steady State

We now briefly sketch the next essential feature of the solutions of the above rotational equations, namely, the approach of the vortex creep to a steady state, say following a glitch, as $\delta\Omega$ tries to heal back to $\delta\Omega_\infty$. The equation for the evolution of the lag $\delta\Omega$ is obtained by combining Eqs. (3.4.4) and (3.4.7) with the expressions involving $\dot{\Omega}_\infty$ given above, and can be expressed in the dimensionless form

$$\frac{dy}{dx} = 1 - \frac{1}{\eta} sinhy \tag{3.4.10}$$

in terms of a dimensionless lag $y \equiv \delta\Omega/\langle\delta\Omega\rangle$, and a dimensionless time co-ordinate $x \equiv \frac{t}{\tau}$, the relevant timescale τ being defined by $\tau \equiv (I_c/I)(\langle\delta\Omega\rangle/|\dot{\Omega}_\infty|) \approx (I_c/I)(kT/E_p)(\delta\Omega_{crit}/\Omega_c)t_s \leq 10^{-5} t_s$. In Eq. (3.4.10), η is the non-linearity parameter, defined as

$$\eta \equiv \frac{r|\dot{\Omega}_\infty|}{4\Omega_s \upsilon_s} exp\{\frac{E_p}{kT}\} \tag{3.4.11}$$

Thus, we expect the solution of Eq. (3.4.10) to have linear and non- linear r'egimes of behavior, depending on the value of η. The physical picture becomes clear when we recognize that the velocity scale for purely thermal motion of vortex lines through the unbiased random potential is given by $v_{th} \sim v_0\ exp(-E_p/kT)$, while that for the steady-state vortex creep dictated by the external spin-down torque is just v_∞, given by Eq. (3.4.8). The parameter η is now readily seen to be the ratio of the two velocity scales, $\eta = (v_\infty/2v_{th})$, or, alternatively, that of the corresponding timescales, $\eta = (t_{th}/2t_s)$, where $t_{th} \equiv (r/2v_{th})$ is the thermal transit timescale. Consider first what happens when $\eta \ll 1$, which means $v_\infty \ll v_{th}$, or, $t_{th} \ll t_s$. The steady-state creep velocity required by the external torque is then small compared to the thermal velocity, and the system can easily set up such a creep rate with only a small bias or lag $\delta\Omega$. This is easily seen by considering the steady-state value y_∞ implied by Eq. (3.4.10), i.e., the value for which dy/dx = 0,

which is obviously $y_\infty = sinh^{-1}\eta$.In the $\eta \ll 1$ limit,this reduces to $y_\infty \approx \eta$, which gives $\delta\Omega_\infty \approx \eta\langle\delta\Omega\rangle$. Thus, on a scale $\langle\delta\Omega\rangle$, the steady-state lag $\delta\Omega_\infty$ is indeed small, and the $\eta \ll 1$ r'egime can be appropriately called the linear r'egime of vortex-creep response.

Consider now the opposite limit, $\eta \gg 1$, in which $v_\infty \gg v_{th}$, and $t_s \ll t_{th}$. Now the external torques require a steady creep rate which is large compared to the thermal velocity, and the systems response changes completely. It can set up such a creep rate only by creating a large bias or lag $\delta\Omega$, which then dominates the whole situation: the systems thermal processes are now driven strongly by the external torque, with interesting and occasionally almost counter-intuitive results [18]. This $\eta \gg 1$ r'egime is the non-linear r'egime of vortex-creep response, in which the value of the steady-state lag $\delta\Omega_\infty$ is given, from the above expression, by $\delta\Omega_\infty \approx ln(2\eta)\langle\delta\Omega\rangle$. We can express this steady lag in the form $\delta\Omega_\infty \approx \delta\Omega_{crit}[1-(kT/E_p)ln(2t_s v_0/r)]$ with the aid of the definitions of η and $\delta\Omega$ given above: this form is, of course, identical to Eq. (3.4.9), showing that $\delta\Omega_\infty \approx \delta\Omega_{crit}$, which is large on a scale $\langle\delta\Omega\rangle$, as anticipated above.

The initial condition to be satisfied by the required solution to the (first order) differential equation (3.4.10) is the specified value of the lag, $\delta\Omega_0$, just after the glitch, i.e., at t = 0.This translates into the condition $y = y_0 \equiv \delta\Omega_0/\langle\delta\Omega\rangle$ at x = 0. The constants appearing in the solution are then y_0 and the steady-state value of y, $y_\infty = sinh^{-1}\eta$. The solution can be expressed in a compact and convenient form by defining a new dependent variable z as:

$$z = tanhy_\infty tanh\frac{y}{2} + sechy_\infty \tag{3.4.12}$$

With the aid of a bit of algebraic manipulation, the solution can be written as:

$$exp(-xcothy_\infty) = \frac{z-1}{z+1}.\frac{z_0+1}{z_0-1} \tag{3.4.13}$$

where z_0 is the value of z at x = 0.

The linear and non-linear limits of the solution (3.4.13) can now be extracted readily. In the linear r'egime, $\eta \approx y_\infty \ll 1$ we need to consider the limit in which the arguments of

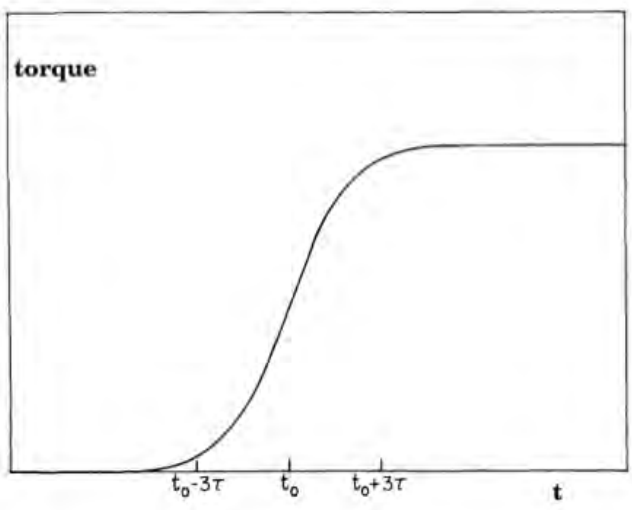

Figure 3.3: Internal torque vs. time (t), showing the characteristic Fermi-function healing.

the hyperbolic functions in Eqs. (3.4.12) and (3.4.13) are all $\ll 1$, so that $tanhu \approx u$ and $sechu \approx 1 - u^2/2$ to the leading order. The algebra is straightforward, and we can easily show that Eqs. (3.4.12) and (3.4.13) respectively reduce to

$$z \approx 1 + \frac{y_\infty}{2}\Big(y - y_\infty\Big), \quad and \quad exp\Big(-\frac{x}{y_\infty}\Big) \approx \frac{y - y_\infty}{y_0 - y_\infty} \tag{3.4.14}$$

in this limit. Rewriting the second equation in (3.4.14) as

$$y = y_\infty + \Big(y_0 - y_\infty\Big) exp\Big(-\frac{x}{\eta}\Big) \tag{3.4.15}$$

we clearly see the characteristics of the solution in this manifestly linear r'egime. First, it depends linearly on the initial perturbation y_0 , as it must [18]. Next, it is a simple exponential approach in time from the initial value y_0 to the steady-state value y_∞, as shown in Fig. 3.3. Finally, the characteristic time of approach in this linear r'egime, $\tau_l = \eta\tau$.

The algebra involved in extracting the non-linear limit, $\eta \gg 1$,is equally straightforward. Now the arguments of the hyperbolic functions in Eqs. (3.4.12) and (3.4.13) are all $\gg 1$, so that the appropriate expressions to the leading order are $tanhu \approx 1 - 2exp(-2u)$ and $sechu \approx 2exp(-u)$, and Eqs. (3.4.12) and (3.4.13) respectively reduce to

$$z \approx 1 + 2(e^{-y_\infty} - e^{-y}), \quad and \quad e^{-x} \approx \frac{e^{-y} - e^{-y_\infty}}{e^{-y_0} - e^{-y_\infty}} \tag{3.4.16}$$

We rewrite the second equation in (3.4.16) as

$$exp(-y) = exp(-y_\infty) + [exp(-y_0) - exp(-y_\infty)]exp(-x) \tag{3.4.17}$$

and note the characteristics of the solution in the non-linear r'egime. First, it has a highly non-linear dependence on the initial perturbation y_0 , as expected. Finally, the characteristic time of approach in this non-linear r'egime is just $\tau_{nl} = \tau$, the timescale.

A remarkable piece of physics emerges from considerations of the response timescales in the linear and non-linear r'egimes. From the definitions of τ, η, t_s and t_{th} given above, we can write the timescale in the linear r'egime as $\tau_l = (1/2)(I_c/I)(kT/E_p)(\delta\Omega_{crit}/\Omega_c)t_{th}$, and that in the non-linear r'egime as $\tau_{nl} = (I_c/I)(kT/E_p)(\delta\Omega_{crit}/\Omega_c)t_s$. The linear response timescale is determined by thermal timescale t_{th} and the non-linear response timescale by the spin-down timescale t_s required by the external torque. This is, consistent with our earlier comment that the non-linear system is driven by the external torque. But the remarkable feature becomes clear when we compare the temperature- dependence of the two timescales. The linear response time scales as $\tau_l \propto (kT/E_p)exp(E_p/kT)$ (remembering that $t_{th} = (r/2v_{th}) = (r/2v_0)exp(E_p/kT)$), so that its behavior is completely dominated by the exponential factor, τ_l becoming rapidly shorter as T increases, i.e., faster relaxation for hotter systems. This is, of course, the expected behavior of thermal relaxation processes. By contrast, the non-linear response time scales as $\tau_{nl} \propto kT/E_p$, implying faster relaxation for colder systems. This appears so counter-intuitive as to be disturbing at first, until we realize that the thermal processes are strongly driven by the external torque in this extreme non-linear limit, as indicated above. The colder the system is, the larger is the steady-state lag or bias required to drive it, and, consequently, the faster is the relaxation towards this steady state.

We have shown above that the linear response is an exponential healing of the lag, so the question now is: is there a correspondingly simple way of characterizing Eq. (3.4.17) for the non-linear response? It turns out that there is such a way, but in terms of the spindown rate, rather than directly in terms of the lag. If we express the spindown rate

of the c-component, $\dot{\Omega}_c$ (which is the observable spindown rate of the star) in terms of its steady- state value $\dot{\Omega}_\infty$. The derivation of this result with the aid of Eqs. (3.4.4), (3.4.10) and (3.4.17), as well as the relations given above Eq. (3.4.8), is straightforward, and the final result:

$$\frac{\dot{\Omega}_c}{\dot{\Omega}_\infty} = \frac{I_s}{I_c}\frac{1}{1+exp[\frac{t-t_0}{\tau_{nl}}]} \tag{3.4.18}$$

Here, t_0 is an offset time [18], which we define as $t_0 \equiv (\delta\Omega_\infty - \delta\Omega_0)/|\dot{\Omega}_\infty|$. To see the physical meaning of the offset time t_0 , consider Eq. (3.4.18), i.e., dimensionless spindown rate vs. time. At the glitch-point, the spindown rate jumps to a value which is $(1 + I_s/I_c)$ times the steady-state rate, and stays essentially constant at this value until a time $\sim t_0$ after the glitch. The crustal superfluid (the s-component) unpins, and so is uncoupled from the external torque, which then acts solely on the c-component for a time $\sim t_0$, raising the spindown rate for this duration. As the above definition of t_0 shows, the lag comes back close to $\delta\Omega_\infty$ at the end of this duration, and the s-component repins on a timescale τ_{nl}. Vortex creep starts again, and the system again approaches a steady state. This persistent shift in the spindown rate following a glitch is thus a signature of strongly non-linear vortex-creep response.

3.5 Stellar Parameters from Glitch Data

Can we attempt to determine structural parameters of neutron stars, and parameters of the essential microscopic physics of their crusts and crustal superfluids, from the data on pulsar glitches in the context of the vortex pinning model, in analogy with what was attempted in the 1970s in the context of the starquake model? Consider first the diagnostic value of observed glitch jumps in essential quantities, e.g., $\Delta\Omega/\Omega$ and $\Delta\dot{\Omega}/\dot{\Omega}$. The former jump does not, by itself,give an essential structural parameter, unlike what happened for the star- quake model, but it can yield valuable results in conjunction with other glitch data, as we shall argue below.

The jump $\Delta\Omega/\Omega$ in the spindown rate is, however, a direct diagnostic in the vortex-pinning model, since we have shown above that this jump is I_s/I_c in this model, and so a direct handle on the fractional moment of inertia of the pinned crustal superfluid. The observed values of $\Delta\Omega/\Omega$ generally lie in the range 10^{-3}–10^{-2} , the large, Vela-type glitches, which constitute the majority, being associated with the largest values of the spindown jump. This indicates the typical moment of inertia of the crustal superfluid to be

$$\frac{I_s}{I_c}\approx\frac{I_s}{I}\sim 10^{-2} \tag{3.5.1}$$

which is a very interesting result.

The above result is directly supported by the recent diagnostic found by Lyne, Shemar and Smith (2000), namely, that, averaged over the observation history of the known glitching pulsars, a fraction $\approx 1.7\times 10^{-2}$ of the spindown amount is reversed by the spinup due to glitch activity. In the vortex-pinning model, the latter spinup is due to the decoupling of the crustal superfluids moment of inertia I_s from the external torque because of unpinning, and hence the above fraction is I_s/I. This yields

$$\frac{I_s}{I}\approx 1.7\times 10^{-2} \tag{3.5.2}$$

in agreement with Eq. (3.5.1).

In fact, the above result can be combined with the observed values of $\Delta\Omega/\Omega$ to obtain diagnostics of the critical lag $\delta\Omega_{crit}$[17]. As the lag $\delta\Omega$ increases with continuing spindown and reaches its critical value, the crustal superfluid unpins suddenly, transferring part or all of its excess angular momentum $I_s\delta\Omega_{crit}$ to the crust rapidly, causing a glitch, i.e., a jump $\Delta\Omega$ in the stellar angular velocity. Hence a lower limit on the critical lag is given by:

$$\frac{\delta\Omega_{crit}}{\Omega}\geq\frac{I}{I_s}\frac{\Delta\Omega}{\Omega}\approx 6\times 10^{-5}\left(\frac{\Delta\Omega}{\Omega}\right)_{-6} \tag{3.5.3}$$

where we have used Eq. (3.5.2) in obtaining the second form of the right- hand side, and $(\Delta\Omega/\Omega)_{-6}$ is the glitch size in units of 10^{-6}. For a value $\Omega\sim 10^2 rads^{-1}$ typical of pulsars

like Vela or Crab, this yields a lower limit $\delta\Omega_{crit} \geq 0.006\ rads^{-1}$ on the critical lag.

There is usually an uncertainty of typically a few weeks in determining the exact glitch-point: if this is $\sim t_0$, as Fig. 3.3 shows, the non-linear Fermi-function healing of the spindown rate can look remarkably similar to a linear, simple- exponential healing if the observations started $\sim t_0$ days after the glitch. Further, a given observation of post-glitch relaxation may require several components, linear and non-linear, and different combinations of components may work equally well. However, the persistent shift in $\dot{\Omega}_c$, which we argued above to be the most convincing signature of non-linear response, does appear to be present in all pulsars for which post-glitch relaxation has been studied in detail, most notably the Crab and Vela pulsars, PSR 0355+54, and PSR 0525+21.

Thus, all pulsars may have non-linear response at least over some parts of their crusts, which brings us to the question of the transition point between linear and non-linear re'gimes. By definition, this point is given by $\eta = 1$, with the aid of the discussion below Eq. (3.4.11), means $t_{th} = 2t_s$, or, $exp(E_p/kT) = 4v_0 t_s/r$. Using $r \sim R$, the stellar radius, we can write the transition value of E_p/kT as:

$$\left(\frac{E_p}{kT}\right)_{trans} = ln\left(\frac{4v_0 t_s}{R}\right) \approx 30.2 + lnt_4 + ln\left(\frac{v_7}{R_6}\right) \tag{3.5.4}$$

where t_4 is t_s in units of 10^4 years, v_7 is v_0 in units of $10^7 cms^{-1}$, and R_6 is R in units of 10^6cm [18].

Only those pinning layers which have E_p/kT greater than this transition value will support non-linear response. Note that the transition criterion depends only logarithmically on the pulsars (spindown) age t_s , but linearly on the temperature T of the inner crust: this determines the effects of aging on the extent of non-linear response in the following, straightforward way. If T remained constant as a pulsar ages, the transition value of E_p would increase slowly, so that, for a given profile of E_p vs. layer density, such as given in Fig. 3.2, the extent of the region of non-linear response would decrease slowly. However, the effects of cooling swamp this trend completely, since E_p decreases linearly with T , and T has a power-law or similar dependence on $|\dot{\Omega}|$ and so on t_s . Thus, the transition value of

E_p actually decreases as the pulsar ages, so that the extent of the non-linearly responding region increases. Physically, as the aging pulsar becomes colder, thermal processes rapidly loss their efficiency, so that strong biases and non-linear response are required over ever-increasing portions of the pinning region in order to meet the demands of the external torque. Younger pulsars like Crab and Vela do, indeed, seem to possess some linearly responding regions; it is possible that these regions shrink with age, becoming negligible in old pulsars [18]. In what follows, we confine ourselves to non-linear response.

The major diagnostic comes from the response time τ_{nl} : combining the earlier expression $\tau_{nl} = (I_c/I)(kT/E_p)(\delta\Omega_{crit}/\Omega_c)t_s$ with Eq. (3.3.6), we obtain

$$\tau_{nl} = \frac{kT}{|\dot{\Omega}_\infty|}.\frac{1}{\rho kr}.\frac{1}{ad}. \tag{3.5.5}$$

If we have an observational limit on T , or a theoretical estimate, a knowledge of τ_{nl} therefore gives a value of ad, which constrains the physics of superfluidity and pinning.

An illustrative example given by Alpar and Pines (1989) is instructive, and we sketch it briefly. If pinning is weak, we can use the statistical arguments for estimating a given in sec. 3.3.2 to obtain a more explicit diagnostic form of Eq. (3.5.5). But the question is: is pinning weak in observed pulsars? These authors argued that it was, since observed upper limits on the critical lag obtained are $\delta\Omega_{crit} \leqslant 0.7\ rads^{-1}$. When combined with the recent lower limit $\delta\Omega_{crit} \geqslant 0.006\ rads^{-1}$ [19], it does suggest that the expected values of the critical lag are much smaller than the early theoretical values described earlier, and far too small to correspond to such strong pinning forces as would be able to pull nuclei out of their lattice sites. We can then use Eq. (3.3.4) for the spacing a between successive pinning centers along the vortex line, and cast Eq. (3.5.5) in a useful diagnostic form with aid of Eq. (3.1.7) for the coherence length d, the definition of the vorticity quantum , the rough estimate of the lattice spacing b given in Eq. (3.3.1), which we simplify here as $\rho b^3 \sim (3A/4\pi)m_B$, and a little straightforward algebra. The form is:

$$\tau_{nl} \sim 40 \frac{T_6 t_4 k_F^{(n)}(fm^{-1})}{E_G(MeV)\Omega_2 R_6} days \tag{3.5.6}$$

where T_6 is T in units of 10^6 K, Ω_2 is Ω in units of 10^2 $rads^{-1}$, other symbols have their previous meanings, and we have used a representative value $A{\sim}200$ for the inner crust.Equation (3.5.6) is a valuable, direct handle on the superfluid energy gap E_G if T can be estimated independently.

Finally, a diagnostic connection between the critical lag $\delta\Omega_{crit}$ and the surface temperature T_s of the neutron star may be possible for old pulsars, in the following way. Vortex creep is a dissipative process. Dissipation of energy during steady-state creep occurs at a rate $\dot{E}_{dis} = I_s\delta\Omega_\infty|\dot{\Omega}_\infty|{\approx}I_s\delta\Omega_{crit}|\dot{\Omega}_\infty|$. This rate would,in general, be added to that of loss of the initial thermal energy content of the neutron star to account for the radiative loss rate $4\pi R^2\sigma T_s^4$ through the surface, and the two contributions would be difficult to separate. However, for old pulsars, we can argue that the initial thermal energy has already been radiated away, and equate the above dissipation rate to the above radiation rate. This yields

$$\frac{\delta\Omega_{crit}}{\Omega_c}{\approx}\frac{2\pi\sigma R^2T_s^4t_s}{E_{rot}(\frac{I_s}{I})}{\sim}10^{-2}\frac{R_6^2T_6^4t_6}{E_{49}(\frac{I_s}{I})_{-2}} \tag{3.5.7}$$

where $E_{rot}{\equiv}(1/2)I\Omega_c^2$ is (roughly) the rotational energy of the star. In Eq. (3.5.7), T_6 is T_s in units of 10^6K, t_6 is t_s in units of 10^6 years, E_{49} is E_{rot} in units of 10^{49}ergs, and the subscript 2 applied to (I_s/I) means its value in units of 10^{-2}.

Although the above equality of rates remains in some doubt, using Eq. (3.5.7) to convert upper limits on the thermal luminosities of radio pulsars to upper limits on the critical lag is a more secure procedure.

Chapter 4

Gravitoelectromagnatism and Measurment of Lense-Thirring Effect

In ordinary circumstance such as terrestrial and include solar system, the gravitational effect can be adequately described to a very degree of accuracy with the Newtonian theory of gravity .Thus it is assumed that the gravitational force depended on the mass of the interacting bodies and their mutual distance only .For a strong gravitational object such as compact stars, it is necessary, to include general relativistic effect [20].

However in general relativity where the space_time curvature plays a fundamental role, neither of these effect is drastiticaly different from the Newtonian theory. For instance the gravitational force, contrary to the Newtonian theory, depends on the velocity of the rotating gravitational source (Lense Thirring effect),on the spin of a relativistic test particle (Desitter precession), generation of gravitational waves etc .Interestingly though these effect have no analogies in the Newtonian theory, these effects have equivalent in the classical electromagnetic theory (induce magnetism, Thomas precession ,electro magnetic wave)

This analogy has been found to be correct provided that the field of the interacting masses is not extremely intense (such as for totally collapsed object Black holes) and the gravitational source is rotating slowly (that is with in the special relativistic limit on the speed). with this approximation it has been shown that the gravitational field equations has equivalent in classical electrodynamics theory in the form of Maxwell's equation and

Lorentz force Law. Hence the approximation is called the gravitomagenetic approximation to the general theory relativity compact stars posses sufficient rotational velocity and enough weak field, hence many process related to these stars can be adequately studied with in the gravitationalelectromagnatic approximation.

On Earth and inside the solar system gravitomagntic effects are extremely small, thus requiring extremely precise measurements so on the other hand the possibility to observe these effect in the strong gravitational field of compact star have been also emphasized especially for the fact that these object naturally posses very high rotational frequencies thus enhancing the typical general relativistic effects.

4.1 The Gravitational Field of a Compact Stellar Source

The gravitational field surrounding a rotating mass differ from that of surrounding a none rotating mass. We can understand this by analogy with the case rotating ,uniformly charged sphere; such a sphere produces both electric and magnetic field whereas a none rotating sphere produces only electric field.

In the general theory of relativity gravitational force is referred to as a manifestation of the curvature of space_time. Thus any process occurring in vicinity of a gravitating source is effective by the geometry of the background space_time. Basic to the geometrical structure of the theory is the general line element given by

$$ds^2 = g_{\alpha\beta} dx^\alpha dx^\beta \tag{4.1.1}$$

Where $g_{\alpha\beta}$ is the matrix tenser defined interms of products of partial derivatives of the coordinate transformation . Physically the component of the metrics tenser($g_{\alpha\beta}$) represent the gravitational field potential in four dimensional space_time .From these component the geometry of the space_time is determined by the distribution of the matter content acting as the source of the gravitational field. This is similar to the electromagnetic field theory where the electromagnetic field is determined by the distribution of charge.

Of a particular important for space_time curvature is the Riemann_ Christoffel curvature tenser defined by equation (1.2.16). Where the Chrestoffel symbol $\Gamma^{\alpha}_{\beta\gamma}$ is related to the metrics tenser by equation (1.3.11)

The fundamental equation of general theory of relativity can now be expressed as

$$R_{\alpha\beta} - \frac{1}{2} g_{\alpha\beta} R = kT_{\alpha\beta} \tag{4.1.2}$$

Where $R_{\alpha\beta}$=$R^{\lambda}_{\alpha\lambda\beta}$ and R= $g^{\alpha\beta}R_{\alpha\beta}$ is the Ricci tenser and Ricci scalar obtained by contraction of the Riemann_Christoffe tenser and k is a constant of proportionality which will be determine in the next sections.

For a non-rotating, un-charged spherically symmetric star of mass M the space_time is given by the Schwarzschild metric as equation 1.4.1. But for a rotating uncharged ,axially symmetric of mass M the metrics has a none vanishing off diagonal component $g_{\varphi t}$= $g_{t\varphi}$ reflecting the conserved angular momentum of the star. For this case the space time is described by Kerr metrics.

$$\begin{pmatrix} (1-\frac{2mr}{\rho^2}) & 0 & 0 & -\frac{2marsin^2\theta}{\rho^2} \\ 0 & \frac{\rho^2}{\Delta} & 0 & 0 \\ 0 & 0 & \rho^2 & 0 \\ -\frac{2marsin^2\theta}{\rho^2} & 0 & 0 & (r^2+a^2+\frac{2mra^2sin^2\theta}{\rho^2})sin^2\theta \end{pmatrix} \tag{4.1.3}$$

Where

$$\rho^2 = r^2 + a^2 cos^2\theta \qquad\qquad \Delta = r^2 + a^2 - 2mr \tag{4.1.4}$$

And the Kerr parameter a=$\frac{J}{M}$ denote the angular momentum of the rotating gravitational source per unit mass

4.2 The Linear Field Approximation

4.2.1 The Newtonian Limit of General Relativity

The motion of a free particle is given by the geodesic equation. Using the proper time τ of the particle as parameter, it takes the form

$$\frac{d^2x^{\mu}}{d\tau^2} + \Gamma^{\mu}_{\alpha\beta}\frac{dx^{\alpha}}{d\tau}\frac{dx^{\beta}}{d\tau} = 0 \tag{4.2.1}$$

Taking the Newtonian limit, $\frac{dx^i}{d\tau} \ll$c (in this section we shall retain the speed of light in the expressions) and keeping only terms to first order in the velocity, we have $d\tau \approx$dt where dt is the usual Newtonian time. Assuming in addition that the metric is diagonal and time independent, the i-component of the acceleration of gravity is found to be

$$g^i = \frac{d^2x^i}{d\tau^2} \approx -\Gamma^i_{00}\frac{d(ct)}{dt}\frac{d(ct)}{dt} = -c^2\Gamma^i_{00} \tag{4.2.2}$$

We have hereby obtained a simple weak-field interpretation of the Christoffel symbols Γ^i_{00}. They represent the components of the acceleration of gravity. Using eq. (1.2.21) and remembering that the metric tensor is assumed to be diagonal, we get

$$\Gamma^i_{00} = -\frac{1}{2}g^{\alpha i}\frac{\partial g_{00}}{\partial x^\alpha} \approx \frac{1}{2}\eta^{ii}\frac{\partial h_{00}}{\partial x^i} = \frac{1}{2}\frac{\partial h_{00}}{\partial x^i} \tag{4.2.3}$$

Inserting this into eq. (4.2.2) we have

$$g^i = \frac{c^2}{2}\frac{\partial h_{00}}{\partial x^i} \tag{4.2.4}$$

This equation shows explicitly how, in the Newtonian limit, the time component of the metric tensor determines the acceleration of gravity.

We will determine the function h_{00} using the field equations. In this case we need only one independent equation, which can be taken as the 00-component of eq. ($R_{\mu\nu}$=k($T_{\mu\nu}$-$\frac{1}{2}Tg_{\mu\nu}$))[26]

$$R_{00} = k\left(T_{00} - \frac{1}{2}g_{00}T\right) \tag{4.2.5}$$

From eq. (1.2.22) we have

$$R_{\mu 0\alpha 0} = \frac{1}{2}\left(h_{\mu 0,0\alpha} - h_{\mu\alpha,00} - h_{00,\mu\alpha} + h_{0\alpha,\mu 0}\right) \tag{4.2.6}$$

Considering a static field, all terms with time derivatives are equal to zero. In this case we get

$$R_{\mu 0\alpha 0} = -\frac{1}{2}h_{00,\mu\alpha} \tag{4.2.7}$$

Contracting μ with α leads to

$$R_{00} = R^\alpha_{0\alpha 0} = -\frac{1}{2}h^\alpha_{00,\alpha} = \frac{1}{2}\frac{\partial}{\partial x^i}\left(\frac{\partial h_{00}}{\partial x^i}\right) \tag{4.2.8}$$

since derivatives with respect to time vanish. Using (4.2.4) this can be written

$$R_{00} = -\frac{1}{c^2}\frac{\partial g^i}{\partial x^i} \tag{4.2.9}$$

In the limit with $h_{\mu\nu} \ll 1$ we can use the Cartesian expression for the divergence so that

$$R_{00} = -\frac{1}{c^2}\nabla.\mathbf{g} \tag{4.2.10}$$

Considering the components of the energy-momentum tensor of a perfect fluid as given by ($T_{\mu\nu}=(\rho + p)u_\mu u_\nu + p g_{\mu\nu}$)[21], we see that in the Newtonian limit the term $T_{00} = \rho c^2$ is dominating. All the other terms can be neglected compared to T_{00} . For the trace of the energy-momentum tensor in the Newtonian limit, we find

$$T = T_0^0 = \eta^{0\alpha} T_{\alpha 0} = T_{00} \tag{4.2.11}$$

This gives

$$T_{00} - \frac{1}{2} g_{00} T \approx T_{00} - \frac{1}{2}\eta_{00} T = \frac{1}{2} T \tag{4.2.12}$$

Equation (4.2.5) can now be written

$$R_{00} = \frac{1}{2} k T_{00} = \frac{1}{2} k \rho c^2 \tag{4.2.13}$$

Equations (4.2.10) and (4.2.13) give

$$\nabla.\mathbf{g} = -\frac{1}{2} k \rho c^4 \tag{4.2.14}$$

This represents the Newtonian limit of Einstein's gravitational field equations in the case of static fields. Comparing equation (4.2.14) with equations (1.1.5) we see that the relativistic equation reduces to the Newtonian gravitational field equations if

$$k = \frac{8\pi G}{c^4} \tag{4.2.15}$$

Thus we have to conclude that the Einstein field equations with the correct constant is

$$R_{\mu\nu} - \frac{1}{2} R g_{\mu\nu} = \frac{8\pi G}{c^4} T_{\mu\nu} \tag{4.2.16}$$

4.2.2 Solutions to the Linearised Field Equations

We shall now consider solutions of the linearised field equations with a non- relativistic mass-distribution as a source. Non-relativistic means that the pressure is so small that it may be neglected compared to the mass density, and the fluid moves so slowly that it is sufficient to include terms of first order in the velocity in the energy-momentum tensor. Einstein's field equations may be written as

$$\Box h_{\mu\nu} = -2k\left(T_{\mu\nu} - \frac{1}{2}\eta_{\mu\nu}T\right) \tag{4.2.17}$$

The solution to this equation can be written as the retarded potential

$$h_{\mu\nu} = \frac{k}{2\pi}\int \frac{[T_{\mu\nu} - \frac{1}{2}\eta_{\mu\nu}T](t', x')}{|\mathbf{x} - \mathbf{x}'|}d^3\mathbf{x}' \tag{4.2.18}$$

where the retarded time, t' , is given by t' = t-$\frac{|\mathbf{x}-\mathbf{x}'|}{c}$. In the following we shall, however, assume that the distances are so small, and the variation of the source so slow, that we may put t' = t. We shall solve the field equations in the presence of a perfect fluid with energy-momentum tensor

$$T^{\mu\nu} = \frac{P}{c^2}g^{\mu\nu} + \left(\frac{P}{c^2} + \rho\right)\frac{dx^\mu}{d\tau}\frac{dx^\nu}{d\tau} \tag{4.2.19}$$

With P=0 and small velocities we get

$$T^{\mu\nu} = \rho\frac{dx^\mu}{dt}\frac{dx^\nu}{dt}, \qquad T = -c^2\rho \tag{4.2.20}$$

so that

$$\begin{aligned} T_{00} - \frac{1}{2}\eta_{00}T &= \frac{1}{2}c^2\rho, \\ T_{i0} - \frac{1}{2}\eta_{i0}T &= -\rho\upsilon^i, \\ T_{ij} - \frac{1}{2}\eta_{ij}T &= \frac{1}{2}\rho\delta_{ij} \end{aligned} \tag{4.2.21}$$

In this case the field equations take the form

$$h_{00} = h_{ii} = \frac{2G}{c^2}\int\frac{\rho}{r}d^3\mathbf{r} = -2\frac{\Phi}{c^2} \tag{4.2.22}$$

there Φ is the Newtonian gravitational potential of eq.($\Phi(r)$=-G$\int \rho(r') \frac{1}{|\mathbf{r}-\mathbf{r}'|} d^3r'$), and

$$h_{i0} = -\frac{4G}{c^2}\int \frac{\rho \upsilon_i}{r} d^3\mathbf{r} = A_i, \qquad h_{ij} = 0, for \quad i \neq j \tag{4.2.23}$$

Here, A_i is the i-component of a vector potential.

Assume that the source is non-rotating and spherically symmetric. Then

$$A_i = -\frac{4G\upsilon_i}{c^2}\int \frac{\rho}{r} d^3\mathbf{r} \tag{4.2.24}$$

4.3 Gravitoelectromagnetism

Gravitomagnetism (sometimes Gravitoelectromagnetism, abbreviated GEM), refers to a set of formal analogies between Maxwell's field equations and an approximation, valid under certain conditions, to the Einstein's field equations for general relativity. According to general relativity, the gravitational field produced by a rotating object (or any rotating mass-energy) can, in a particular limiting case, be described by equations that have the same form as the magnetic field in classical electromagnetism. Starting from the basic equation of general relativity, the Einstein field equation, and assuming a weak gravitational field or reasonably flat space_time, the gravitational analogs to Maxwell's equations for electromagnetism, called the GEM equations, can be derived. The solution of the field equation may be written in terms of retarded potentials as

$$\bar{h}_{\mu\nu} = \frac{k}{2\pi}\int \frac{T_{\mu\nu}(t - \frac{|\mathbf{x}-\mathbf{x}'|}{c}, \mathbf{x}')}{|\mathbf{x}-\mathbf{x}'|} d^3\mathbf{x}' \tag{4.3.1}$$

where $\mathbf{x}$ is a spatial vector and $T_{\mu\nu} = T_{\mu\nu}$(t, $\mathbf{x}$). The energy-momentum tensor $T\mu\nu$ mimics the behaviour of an electromagnetic four-current J_μ and the tensor potential $\bar{h}_{\mu\nu}$ mimics a field potential A_μ.

We shall assume that the energy-momentum tensor obeys $|T_{00}| \gg |T_{ij}|$ and $|T_{0i} \gg |T_{ij}$ in the weak field approximation.Hence from eqn.(4.3.1) $|h_{00}| \gg |\bar{h}_{ij}|$ and $|\bar{h}_{0i}| \gg |\bar{h}_{ij}|$ Then we can write

$$\bar{h}_{00} = -\frac{4\Phi}{c^2} \tag{4.3.2}$$

$$\bar{h}_{0i} = \frac{2A_i}{c^2} \tag{4.3.3}$$

Here, Φ is the Newtonian or gravitoelectric potential

$$\Phi = -\frac{GM}{r} \tag{4.3.4}$$

and A_i is the gravitomagnetic vector potential given in terms of the total angular momentum S of the system

$$A_i = \frac{G}{c}\frac{S^j x^k}{r^3}\varepsilon_{ijk} \tag{4.3.5}$$

The mass m is related to the mass-density $\rho = \frac{T_{00}}{c^2}$ by

$$\int \rho d^3\mathbf{x} = m \tag{4.3.6}$$

and the angular momentum S to the mass-current density $j^i = \frac{T_{0i}}{c}$ by

$$S^i = 2\int \varepsilon^i_{jk} x^j j^k d^3\mathbf{x} \tag{4.3.7}$$

The Lorenz gauge condition $\bar{h}^{\mu\alpha}_{,\alpha}=0$ can be written in terms of the potentials Φ and A

$$\frac{1}{c}\frac{\partial \Phi}{\partial t} + \frac{1}{2}\nabla.\mathbf{A} = 0 \tag{4.3.8}$$

This is, apart from a factor $\frac{1}{2}$, the Lorenz gauge condition in electromagnetism. This factor relates to the fact that the electromagnetic field is a spin-1 field, while the geometrodynamical field involves a spin-2 field. Defining the gravitoelectric and gravitomagnetic fields E_G and B_G by

$$\mathbf{E}_G = -\nabla\Phi - \frac{1}{2c}\frac{\partial A}{\partial t} \tag{4.3.9}$$

$$\mathbf{B}_G = \nabla x \mathbf{A} \tag{4.3.10}$$

It then follows from the gravitational fields equations and the Lorentz gauge condition that for a slowly rotating gravitating mass[16].

‘GEM equations Maxwell’s equations

$$\nabla.\mathbf{E}_G = -4\pi G\rho \qquad \nabla.\mathbf{E} = \frac{\rho_{em}}{\epsilon_0} \tag{4.3.11}$$

$$\nabla.\mathbf{B}_G = 0 \qquad \nabla.\mathbf{B} = 0 \tag{4.3.12}$$

$$\nabla\times\mathbf{E}_G = -\frac{1}{2c}\frac{\partial B_G}{\partial t} \qquad \nabla\times\mathbf{E} = -\frac{\partial B}{\partial t} \tag{4.3.13}$$

$$\nabla\times\frac{1}{2}\mathbf{B}_G = -\frac{4\pi G}{c}j + \frac{1}{c}\frac{\partial E_G}{\partial t} \qquad \nabla\times\mathbf{B} = \frac{1}{\epsilon_0 c^2}\mathbf{J} + \frac{1}{c^2}\frac{\partial E}{\partial t} \tag{4.3.14}$$

These are the Maxwell equations for the gravitoelectromagnetic (GEM) fields in comparison with the Maxwell equations of electromagnetism.

These fields describe the space_time outside a rotating object in terms of the gravitoelectric and gravitomagnetic fields. For a test particle whose mass m is small in a stationary system, the net (Lorentz) force acting on it due to a GEM field is described by the following GEM analog to the Lorentz force equation:

$$\mathbf{F}_m = m(\mathbf{E}_g + \mathbf{v}\times 2\mathbf{B}_g) \tag{4.3.15}$$

where: m is the mass of the test particle; $\mathbf{v}$ is the instantaneous velocity of the test particle. Acceleration of any test particle is simply:

$$\mathbf{a} = \mathbf{E}_g + \mathbf{v}\times 2\mathbf{B}_g \tag{4.3.16}$$

In some literature, all instances of B_g in the GEM equations are multiplied by $\frac{1}{2}$,factor absent from Maxwells equations. This factor vanishes if B_g in the GEM version of the Lorentz force equation is multiplied by 2, as shown above. The factors 2 and $\frac{1}{2}$ arise because gravitational field is caused by stress-energy tensor which is second rank tensor, as opposed to electromagnetic field which is caused by four-current which is first rank tensor. That difference becomes intuitively clear when non-invariance of relativistic mass is compared to electric charge invariance. This is often referred to as gravity being spin-2 field and electromagnetism being spin-1 field.

4.4 Gravitomagnetic Fields of Astronomical Objects

Formula for gravitomagnetic field B_g near a rotating body can be derived from the GEM equations and is:

$$\mathbf{B}_g = \frac{G}{2c^2}\frac{\mathbf{L} - 3(\mathbf{L}.\mathbf{n})\mathbf{n}}{r^3} \tag{4.4.1}$$

Where $\mathbf{n}$ is the unit vector in the radial direction $\mathbf{n}=\frac{\mathbf{r}}{r}$ and $\mathbf{L}$ is the angular momentum of the body.At the equlaterial plane,$\mathbf{r}$ and $\mathbf{L}$ are perpendicular,so their dot product vanishes,and this formula reduces to:

$$\mathbf{B}_g = \frac{G}{2c^2}\frac{\mathbf{L}}{r^3} \tag{4.4.2}$$

Magnitude of angular momentum of a homogeneous ball-shaped body is:

$$L = I_{ball}w = \frac{2mr^2}{5}\frac{2\pi}{T} \tag{4.4.3}$$

Where:$I_{ball} = \frac{2mr^2}{5}$ is the moment of inertia of a ball-shaped body; w is the angular velocity;m is the mass; r is the radius;T is the rotational period.Therefore,magnitude of Earth‘s gravitomagnetic field at its equator is:

$$\mathbf{B}_{g_{earth}} = \frac{G}{5c^2}\frac{m2\pi}{rT} = \frac{2\pi Rg}{5c^2T} \tag{4.4.4}$$

Where $g=\frac{GM}{r^2}$ is the Earth‘s gravity. From this calculation it follows that Earths equatorial gravitomagnetic field is about $B_{g_{earth}}$=1.012$\times 10^{-14}$Hz, [14] or 3.1 $\times 10^{-7}$ in units of standard gravity (9.81 $\frac{m}{s^2}$) divided by speed of light. Such a field is extremely weak and requires extremely sensitive measurements to be detected. If the preceding formula is used with the second fastest-spinning pulsar , PSR J1748- 2446ad (which rotates 716 times per second),assuming a radius of 16km, and two solar masses, then the gravitomagnetic field is about 166 Hz. This would be easy to notice

4.5 Lense-Thirring Effect

Particles orbiting a rotating body (like the Earth), will experience a gravitomagnetic field which will make their orbit precess. This precession is called the Lense-Thirring effect in

honour of the physicists Josef Lense and Hans Thirring who first predicted this effect in 1918 [LT18].

The Lense-Thirring precession can be calculated by examining the equation of motion of a particle in the gravitational field(4.1.3). However the calculation is rather complicated ,and much simpler to obtain the answer by exploitation the analogy between the gravitational and electromagnatic equations.

The Lense-Thirring precession is analogous to the precession of orbital angular momentum of a charged particle orbiting around another charged particle endowed with a magnetic dipole moment[2]. The time average magnetic moment $\mathbf{m}$ associated with the angular momentum of the orbiting particle then couples to the magnetic dipole moment $\mathbf{m}'$ of the central particle, via the magnetic field, and this results in an effective torque on the orbital angular momentum. The magnetic field of the dipole $\mathbf{m}$ is given by the familiar formula

$$\mathbf{B} = \frac{3\mathbf{nn}.\mathbf{m} - \mathbf{m}}{r^3} \tag{4.5.1}$$

the torque exerted by the magnetic field on the dipole $\mathbf{m}'$ is

$$\tau = \mathbf{m}' \times \frac{3\mathbf{nn}.\mathbf{m} - \mathbf{m}}{r^3} \tag{4.5.2}$$

By analogy the torque exerted by the gravimagnetic field on the orbital angular momentum is

$$\tau = -\mathbf{GL} \times \frac{3<\mathbf{nn}.\mathbf{m}> - \mathbf{m}}{r^3} \tag{4.5.3}$$

The torque is, as usual, equal to the time derivative of the angular momentum, and hence,

$$\frac{d\mathbf{L}}{dt} = -\mathbf{GL} \times \frac{3<\mathbf{nn}.\mathbf{s}> - \mathbf{s}}{r^3} \tag{4.5.4}$$

from which using the formula $\frac{d\mathbf{L}}{dt} = \mathbf{\Omega} \times \mathbf{L}$ we can read off the precession angular velocity as

$$\Omega = -G\frac{3<\mathbf{nn}.\mathbf{s}> - \mathbf{s}}{r^3} \tag{4.5.5}$$

If the polar orbit is of low altitude (r=R_E) , the magnitude of the Lense-Thirring precession amount to about 0.05 arcsec per year

Chapter 5

Result and Discussion

The gravitational redshift at a neutron star surface is $\sim$0.3, and therefore relativistic effects, including the dragging of the inertial frames(Lense-Thirring Effect), are strong in and around neutron stars. In this section we analyze how frame dragging affects the relative precession of the crust and the core. To find the Gravitomagnetic coupling torque on the crust of the neutron star by the core; Consider the gravitomagnetic force acting on a small region of the crust of mass dm. In the post-Newtonian approximation, it is given by

$$dF_{gm} = dm\mathbf{v}\times\mathbf{B}_g = dm(\Omega_\mathbf{c}\times\mathbf{r})\times\mathbf{B}_g \tag{5.0.1}$$

where v, B_g , Ω_c , and r are the velocity of the small region, the gravitomagnetic field, the instantaneous angular velocity of the crust, and the radius vector of the region, respectively. The torque acting on this region of the crust is given by

$$d\tau = \mathbf{r}\times dF_{gm} = dm(\mathbf{r}\times(\Omega_\mathbf{c}\times\mathbf{r})\times\mathbf{B}_g) \tag{5.0.2}$$

using the vector identity

$$(\mathbf{A}\times\mathbf{B})\times\mathbf{C} = (\mathbf{C}.\mathbf{A})\mathbf{B} - (\mathbf{C}.\mathbf{B})\mathbf{A} \tag{5.0.3}$$

$$d\tau = dm(\mathbf{B}_g.\mathbf{r})(\Omega_\mathbf{c}\times\mathbf{r}) \tag{5.0.4}$$

The field B_g is that of a dipole[26], and

$$\mathbf{B}_g.\mathbf{r} = -\frac{6}{r^3}\mathbf{J}.\mathbf{r} = -\frac{6I_0}{r^3}\Omega_\mathbf{0}.\mathbf{r} \tag{5.0.5}$$

where J, Ω_0, and I_0 are the angular momentum, the angular velocity, and the moment of inertia of the spherical core,

Now, substituting equation (5.0.5) into equation (5.0.4) and integrating over the crust, we arrive at the following form of the gravitomagnetic torque: respectively

$$\tau = -\int \rho d^3\mathbf{r}\left[\left(\frac{6I_0}{r^3}\right)\Omega_{\mathbf{0}}.\mathbf{r}\right](\Omega_{\mathbf{c}}\times\mathbf{r}) \tag{5.0.6}$$

$$\tau = \Omega_{\mathbf{c}}\times I_g\Omega_{\mathbf{0}} \tag{5.0.7}$$

where I_g is the linear operator (represented, generally, by a 3×3 matrix) defined as

$$I_g\Omega_{\mathbf{0}} = -\int \rho d^3\mathbf{r}\left(\frac{6I_0}{r^3}\right)(\Omega_{\mathbf{0}}.\mathbf{r})\mathbf{r} \tag{5.0.8}$$

We use Diracs bra and ket notation and express this operator as

$$I_g = -\int \rho d^3\mathbf{r}\left(\frac{6I_0}{r^3}\right)|\hat{r}><\hat{r}| \tag{5.0.9}$$

Where we define the projection operator $|\hat{r}><\hat{r}|$— by its action on an arbitrary vector $\mathbf{a}$:

$$(|\hat{r}><\hat{r}|)\mathbf{a} = (\mathbf{r}.\mathbf{a})\mathbf{r} \tag{5.0.10}$$

From equation (5.0.9) we see that I_g is a Hermitian operator: since the integrand $\propto|\hat{r}><\hat{r}|$ in equation (5.0.9) is Hermitian, the integral must also be Hermitian.This means that the matrix representing I_g is symmetric. If the crust is spherically symmetric, then I_g = zI, where z is a real number and I is a unit matrix. In this case, the torque acting on the crust is

$$\tau = z\Omega_c\times\Omega_0 \qquad\qquad z\simeq\mathbf{I}_c\mathbf{I}_0\left(\frac{2G}{c^2R^3}\right) = 0.1I_c \tag{5.0.11}$$

This torque term arises from gravitational dragging, which gives place to a retardation of the angular velocity of the crust components of the star ,when it has a different angular velocities from the core. But only the φ component of the torque is responsible for the retardation of the angular velocity of the crust, If the crust is rotating along the φ. For simplicity; if we decompose the torque using cylindrical coordinate, we will get

$$\tau = z\Omega_{c\phi}\Omega_0\hat{\rho} - z\Omega_{c\rho}\Omega_0\hat{\phi} \tag{5.0.12}$$

So the ϕ component of the torque is

$$\tau_{\phi} = -z\Omega_c\Omega_0 sin\theta \tag{5.0.13}$$

Where θ is the angle between Ω_c and Ω_0 ,its value as shown on the observation is very small but not zero ($\sin\theta \simeq \theta$). Using the above expression we can determine the time when both the core and the crust have the same speed

$$t_{syc} = \frac{I_c}{\tau_{\phi}}(\Omega_c - \Omega_0) \simeq \frac{I_c}{z\Omega_c\Omega_0\theta}(\Omega_c - \Omega_0) \tag{5.0.14}$$

After this time both the crust and the core rotate with the same angular velocity. For example, if we consider the Crab pulsar, for which[23], $\Omega_c = 2001/s$, $\Omega_0 = 1001/s$ and $\theta = 10^{-14}$, $t_{sys} = 1.58\times10^3$years.

Chapter 6

Conclusion

As we have discussed,an interesting consequence of the pinning of vortice's on fluxoids is the lag between the angular velocity of the core superfluid and the crust - unlike in the case where there is no pinning, the superfluid will be rototating faster than the crust in the steady state. As the magnetic field is expelled from the core, pinning force per unit length of the vortex will decrease. Consequently, the steady state lag between the core superfluid and the crust will decrease till eventualy it will practically vanish as the pinning force per unit length of the vortex becomes negligible. Thus, during the first lo^6 years or so one has a reservoir of angular momentum residing in the core superfluid. We have argued that if the lag decreases in a series of discontinuous steps then it provides an alternative or additional mechanism for sudden spin-up of the crust as observed in glitches. We have also argued that if at all relevant this is more likely to happen in older pulsars.

Glossary

Ambient Superfluid→is a state of matter in which the matter behaves like a fluid with zero viscosity.

Coherence length→is the propagation distance from a coherent source to a point where an electromagnetic wave maintains a specified degree of coherence.

Energy gap→ is a finite energy difference betweeen ground state and first excited states.

Fermi surface→a constant-energy surface in the space containing the wave vectors of states of members of an assembly of independent fermions.

Fermions→ are elementary particles which have half spin.

Fluxoids→ are magnetic flux of vortices.

Gyroscope→is a device for measuring or maintaining orientation, based on the principles of angular momentum.

Manifolds→are isotropic, meaning that the geometry on the manifold is the same regard less of direction.

Pinning→ means, that the normal core regions of the vortex lines would prefer to pass through the positions of the crustal nuclei on the lattice sites, and would stay fixed in this manner.

Post-glitch relaxation→is a process of recoupling the creep to another steady state.

Retarded potential→the scalar or vector potential of a time varying current or charge distribution.

Tides→ are the manifestation of a gradient of the gravitational force field induced by a mass above an extended body or a system of particles.

Vortices→ are parallel arrays of superfluids which carry much of the interior angular momentum.

Vortex creep→ is a quantum tunneling between adjacent sites which are geometrically suitable for pinning.

Bibliography

[1] C. Porciani, A. Dekel, and Y. Hoffman, Testing tidal-torque theory: I. Spin amplitude and direction - Testing tidal-torque Theory: II. Alignment of inertia and shear, and the characteristics of proto-haloes, MNRAS 332, 325351 (2002).

[2] Ohanian H.C and Ruffini R,Gravitation and Spacetime,W.W.Norton and comp pany, second, Edition,1994.

[3] B. F. Schutz, .An Introduction to General Relativity., Cambrige Univ. Press, Cambridge UK (1984).

[4] Lucieno Rezzolla.Lecter on Geodisc Devation and Weak field solution ,SISSA,International school for advanced studies and INFN,Triete Italy,(2004).

[5] Feynman, R. P., Metropolis, N. and Teller, E. (1949), Equations of state of ele ments based on the generalized Fermi-Thomas theory, Phys. Rev., 75,1561.

[6] Ruderman, M. (1969), Neuton Starquakes and Pulsar Periods, Nature, 223,597, Ruderman et al.,1998.

[7] Anderson, P. W., Alpar, M. A., Pines, D. and Shaham, J. (1982), The rheology of neutron stars: vortex-line pinning in the crust superfluid, Phil. Mag. A, 45, 227.

[8] Baym, G. and Pines, D. (1971), Neutron starquakes and pulsar speedup, Ann. Phys., 66, 816.

[9] Ghosh, P. (1994), Spin evolution of neutron stars in accretion powered pulsars, in The evolution of X-ray binaries, eds. S. S. Holt and C. S. Day, AIP conference series, New York, 308, 439.

[10] Anderson, P. W. and Itoh, N. (1975), Pulsar glitches and restlessness as a hard superfluidity phenomenon, Nature, 256, 25.

[11] Migdal, A. B. (1959), Superfluidity and the moments of inertia of nuclei, Zh. Eksp. Teor. Fiz., 37, 249, also in Soviet Phys.-JETP, 10, 176.

[12] Baym, G. (1970), Neutron stars, Lectures given at the Niels Bohr institute and NORDITA, Copenhagen, NORDITA publ.

[13] Hoffberg, M., Glassgold, A. E., Richardson, R. W. and Ruderman, M. (1967), Anisotropic superfluidity in neutron star matter, Phys. Rev. Lett., 24,775.

[14] Onsager, L. (1949), Statistical hydrodynamics, Nuovo Cimento Suppl., 6, 279.

[15] Pines, D. (1971), Inside neutron stars, in Proc. 12th international conference on low-temperature physics, ed. E. Kanda, Acad. Press Japan, Tokyo, p. 7.

[16] Alpar, M. A., Anderson, P. W., Pines, D. and Shaham, J. (1984), Vortex creep and the internal temperature of neutron stars. I. General theory, Astrophys.J.,276, 325.

[17] Alpar, M. A. (1977), Pinning and threading of quantized vortices in the pulsar crust superfluid, Astrophys. J., 213, 527.

[18] Alpar, M. A. and Pines, D. (1989), Vortex creep dynamics: "Theory and observation, in Timing neutron stars, eds. H. Ogelman and E. P. J. van den Heuvel, Kluwer, Dordrecht, p. 441.

[19] Lyne, A. G., Shemar, S. L. and Smith, F. G. (2000), Statistical studies of pulsar glitches, Mon. Not. Roy. Astron. Soc., 315, 534.

[20] C.W. Misner, K. S. Thorne and J. A. Wheeler, .Gravitation., Freeman, NY (1974).

[21] Winberg S.:Gravitation and cosmology and application of the general theory of relativity John Willay,Newyork,(1972).

[22] Gravitomagnetic Effects on a plasma surrounding a slowly rotating compact star Barur.M.Mirza-Quaid-I-Azam University,Islamabad,Pakistan

[23] arXiv:astro ph/9801070v1 9 Jan 1998.

Declaration

This thesis is my original work, has not been presented for a degree in any other University and that all the sources of material used for the thesis have been dully acknowledged.

Name: Asfaw Merid

Signature:– – – – – – – – – – –

Place and time of submission: Addis Ababa University, June 2013

This thesis has been submitted for examination with my approval as University advisor.

Name: Dr. Legesse Wetro

Signature:– – – – – – – – ––